ISSN 0869-5911, Petrology, 2006, Vol. 14, No. 5, pp. 423–451. © Pleiades Publishing, Inc., 2006.
Original Russian Text © S.P. Korikovsky, L.I. Khodorevskaya, 2006, published in Petrologiya, 2006, Vol. 14, No. 5, pp. 453–481.

Granitization of Paleoproterozoic High-Pressure Metagabbro-Norites of the Belomorian Group in Gorelyi Island, Kandalaksha Bay Area, Baltic Shield

S. P. Korikovsky[a] and L. I. Khodorevskaya[b]

[a] *Institute of the Geology of Ore Deposits, Petrography, Mineralogy, and Geochemistry (IGEM), Russian Academy of Sciences, Staromonetnyi per. 35, Moscow, 109017 Russia*

e-mail: korik@igem.ru

[b] *Institute of Experimental Mineralogy, Russian Academy of Sciences, Chernogolovka, Moscow oblast, 142432 Russia*

e-mail: lilia@iem.ac.ru

Received January 20, 2006

Abstract—The process of granitization was studied in a small massif of high-pressure Paleoproterozoic (2.45–2.36 Ga) metagabbro–norites (coronites) of the Belomorian Group at contacts with *Bt-Hbl-Kfs-Pl-Qtz* gneiss-granites. The granitization process occurred at the culmination of Svecofennian metamorphism, at T = 660–700°C and P = 9.5–10.5 kbar. The process affected the marginal portion (15–20 m thick) of the massif and proceeded under the effect of silicic–alkaline H_2O–Cl–CO_2 fluids related to the gneiss–granites and was of infiltration nature. The metagabbroids became enriched in Na, K, Si, Cl, CO_2, and H_2O and depleted in Ca, Mg, Fe, and Cr, which were removed outside the reaction zone. The debasified metabasites underwent melting during the final stages of the process. The changes in the bulk-rock compositions became more intense closer to the contact with the gneiss-granite, as can be clearly seen in the variation diagrams. Before their transformations, the metagabbroids contained magmatic minerals: pigeonite, pigeonite-augite, high-Ti biotite, and labradorite-bytownite, which are partly replaced by metamorphic minerals (sometimes in the form of reaction coronas): garnet, clinopyroxene, orthopyroxene, magnesian hornblende, anthophyllite, biotite, and andesine. According to the changes in the phase relations and the composition of the rocks, the contact–reaction interval can be subdivided into the following four zones: (I) weakly amphibolized metagabbro-norite; (II) apogabbro *Hbl–Pl* ± *Scp* ± *Qtz* plagioamphibolites with rims, and then with pseudomorphs, after magmatic and corona minerals; (III) K-feldspathized *Hbl–Bt–Pl–Kfs* ± *Scp–Qtz* apogabbro amphibolites; and (IV) gneiss-granites with skialiths of bleached *Bt–Hbl–Pl–Kfs* ± *Scp–Qtz* amphibolites. Zone I contains newly formed embryonic *Hbl*, *Opx*, and *Ath* reaction rims around magmatic and coronitic minerals. In zone II, *Pig*, *Pig-Aug*, and *Grt* are completely replaced by hornblende and anthophyllite, and *Lbr* is replaced by andesine and scapolite with a calcite admixture. In zone III, *Hbl* is further replaced by biotite; andesine is replaced by oligoclase, potassic feldspar, and quartz; and *Ath* and *Opx* are decomposed. Biotitization becomes more intense in zone IV, where *Hbl* and *Bt* are partly replaced by feldspars and quartz, which mark the maximum of the debasification and enrichment in alkalis of the metagabbro-norites. The paper presents descriptions of reaction textures and mineral reactions that mark the transitions between the zones and considers the stability conditions of *Ath* and *Opx* in zones I and II and the causes of the disappearance of these minerals from zones III and IV. Equilibria of the *Pl–Scp* pair are discussed. The variations in the compositions of minerals from zone I through zone IV are systematic and display clearly pronounced tendencies. The hornblende becomes progressively more ferrous (its iron mole fraction increases from 0.31 to 0.69), along with an increase in the concentrations of alkalis and the K/Na ratio. The biotite also becomes more ferrous (from 0.28 to 0.61) and depleted in Ti in comparison with magmatic biotite. The anorthite content in plagioclases decreases from 60–80 to 20–22%. The content of the meionite end member in the scapolite varies from 30 to 50% but depends not on the zone but on the CO_2 and Cl concentrations in the fluid. The distribution of the *Me* and *An* end members between *Scp* and *Pl* is equilibrium. Calculations indicate that the fluid in the most strongly transformed rear zone IV was a highly concentrated carbon dioxide–chloride brine rich in alkalis and silica. The transformations of the gabbroids in zones I–III was of metasomatic character. Zone IV is marked by the onset of the fragmentation of the amphibolized and bleached metagabbro-norites, their transformation into skialiths submerged into gneiss-granite, and their further debasification and enrichment in alkalis. This process ends with the progressively more intense melting and dissolution of the nebular remnants of the metabasites in the anatectic granite migma or magma. The aureole described in this publication makes it possible to trace all granitization stages in metagabbroids in compliance with the known model proposed by D.S. Korzhinskii.

DOI: 10.1134/S086959110605002X

INTRODUCTION

The process of anatectic formation of granitoids can be explained within the framework of two models: anatexis in a closed system and granitization, with these models differing, first and foremost, in the assumed roles and sources of fluids in this process. The classic model of in-situ anatexis admits that the fluids can be provided only by the processes of the dehydration and decomposition of aqueous minerals, first of all, micas and amphiboles at a temperature maximum, which is believed to be the principal reason for anatexis itself (Mehnert, 1968). In contrast, the model of granitization, which was developed in much detail by D.S. Korzhinskii (1952), explains the melting of all rock types by the action of flows of deep silicic–alkaline fluids at a metamorphic culmination, a process that causes the debasification and alkali enrichment of the rocks and their ensued progressively more extensive partial and, eventually, complete melting. In fact, both models are anatectic, but the former considers the process in a closed system, while the latter assumes that the system is open.

This publication is based on our results obtained for a field of rocks of the Belomorian series in the Baltic Shield and is centered on the reaction relations of the synmetamorphic granitoids and fluids related to these rocks with corona-bearing metagabbro-norites under amphibolite-facies conditions. The action of fluid on the gabbroids was an infiltration-controlled process, in complete consistence with D.S. Korzhinskii's (1952, 1976) model, which was later further developed by V.A. Zharikov, S.N. Gavrikova, F.A. Letnikov, S.P. Korikovsky, L.L. Perchuk, and other petrologists (Zharikov, 1987, 1996; Zharikov and Gavrikova, 1987; Gavrikova and Zharikov, 1984; Korikovsky, 1967; Letnikov et al., 1988, 2000; Perchuk, 1987). In complete agreement with this model, the frontal inflow of silica and alkalis into the Belomorian metagabbro-norites from the gneiss-granites caused the replacement of magmatic and metamorphic pyroxenes and garnets by hornblende and biotite and the replacement of magmatic labradorite, bytownite, and partly amphibole and biotite by andesine, oligoclase, quartz, potassic feldspar, and scapolite. This process was responsible for the metasomatic alkali enrichment and the debasification of the marginal portion of the metagabbro–norite massif. The transformations became more intense closer to the granite, so that the originally quartz-free metagabbroids were transformed first into homogeneous but still massive quartz- and potassic feldspar-bearing amphibolites. In immediate contact with the gneiss-granite, these rocks are disintegrated, and their fragments are detached from the main metagabbro-norite body and transformed into isolated nebular skialiths in gneiss-granite, with these skialiths eventually completely dissolving in the gneiss-granite. There are no discernible traces of either the contact hybridism of the granites or the nearby redeposition of leached Ca, Mg, and Fe from the percolating fluids, facts testifying that these components were completely removed outside the reaction zone and then disseminated. Analogous processes of the active debasification of metabasites and their eventual replacement by granite melt are typical of migmatite and granite-gneiss fields under amphibolite- and granulite-facies conditions, and granitization under the effect of silicic–alkaline brines is the most widely spread and ubiquitous mechanism that produces acid anatectic magmas (Korzhinskii, 1976). Some mineralogical and petrochemical aspects of this process are discussed in this publication using the example of granitization in a metagabbro-norite massif in the Belomorian Complex.

The Archean Belomorian series consists of a diversity of migmatized biotite, biotite–garnet, and kyanite–garnet–mica gneisses with intercalations of hornblende, garnet, and clinopyroxene amphibolites (Volodichev, 1990) and with numerous bodies of Paleoproterozoic (2.45–2.46 Ga) gabbro-norites (Sharkov et al., 2004), which were metamorphosed together with their host rocks and acquired reaction coronitic (so-called drusite) textures. Bibikova et al. (2004) summarized all available isotopic dates of the Belomorides and demonstrated that the emplacement of the gabbroids into the Archean sequence and the Svecofennian cycle at 1.85–1.9 Ga were separated by a long-lasting (about 500 m.y.) interlude devoid of any processes of metamorphism or granite formation in the Belomorian Complex. This interlude was terminated by the Svecofennian metamorphic event with the origin of attendant gneiss-granites and pegmatites. During this cycle, the Archean rocks were extensively recrystallazed, and the supracrustal Belomorian sequences underwent prograde metamorphism. This cycle also produced apogabbro coronites, whose Sm–Nd mineral age is ~1.9 Ga (Alekseev et al., 1999).

Phase relations during the regional metamorphism of the Belomorian Group and the coronitization of the gabbroids corresponding to the high-temperature amphibolite facies were studied fairly exhaustively (Volodichev, 1990; Larikova, 2000; and others). At the same time, the interaction of numerous granitoid veins penetrating the Belomorian rocks and the coronitic metagabbro have never been examined in detail as of yet. To bridge this gap, we studied gneiss-granites that belong to the vein series of the migmatized gneiss–amphibolite complex in contact with a massif of coronitic metagabbro (so-called drusites), which are typical of the Belomorides and are exposed, for example, in Gorelyi Island in Kandalaksha Bay.

REGIONAL METAMORPHISM OF GABBRO-NORITES AND THEIR HOST ROCKS

The gabbroids compose a small (150–250 m in diameter) equant massif hosted by biotite and biotite–garnet gneisses with lenses of ordinary garnet–clinopy-

roxene, garnet, and anthophyllite-bearing amphibolites. The metamorphic mineral assemblages of the host rocks (*Grt + Cpx + Hbl + Pl + Qtz*, *Hbl + Pl + Qtz*, *Grt + Hbl + Ath + Bt + Pl + Qtz*, *Hbl + Cpx + Pl + Qtz*, *Hbl + Ath + Pl + Qtz*, *Bt + Grt + Pl + Qtz*, and others) are equilibrated and display evidence of their prograde evolution.[1] These traces of prograde metamorphism are revealed when large (up to 2 cm in diameter) garnet crystals are examined: they are either homogeneous or have smooth prograde zoning practically throughout the whole profiles across these grains, with X_{Mg} increasing by 5–7% toward grain margins. Garnet grains sometimes possess very thin (no thicker than 15–20 μm) outermost retrograde zones. The prograde character of metamorphism of the rocks also follows from the fact that the cores of garnet grains contain epidote inclusions, which are relics of an earlier metamorphism to the epidote-amphibolite facies, whereas the outer zones of the same garnet crystals have inclusions mostly of hornblende, clinopyroxene, and plagioclase. The matrix clinopyroxene coexisting with the garnet and pyroxene inclusions in the garnet are augite containing 5–8% *Jd*. The identity of the *Grt–Cpx–Hbl–Pl* assemblage of the amphibolites and the obviously Svecofennian *Grt–Cpx–Hbl–Pl* coronitic associations of the metagabbro (see below), the compositional similarities between the analogous minerals and their crystallization temperatures indicate that the processes had the same age and analogous *P–T* parameters. The prograde character of the metamorphic evolution of the host Archean rocks demonstrates that the metamorphic grade of the Svecofennian metamorphism in this area was higher than the grade of the Archean metamorphism. The *Grt–Hbl* and *Grt–Cpx* mineralogical thermometry of the amphibolites with the use of progradely zoned garnet porphyroblasts and hornblende and clinopyroxene inclusions in them (Korikovsky, 2005) yields temperatures of 520–580°C **for garnet cores** (epidote-amphibolite facies). **The peak temperature,** determined by the outer prograde rims of garnet and matrix hornblende (or clinopyroxene), varies from 640 to 660°C according to the *Grt–Hbl* thermometer (Perchuk, 1989) or from 670 to 710°C according to the *Grt–Cpx* thermometer (Powell, 1985). The *Grt–Hbl–Pl–Qtz* and *Grt–Cpx–Pl–Qtz* barometry of the amphibolites based on the compositions of the same minerals and plagioclase coexisting with them yielded pressures of 9.6–10.5 kbar (Kohn and Spear, 1990; Eckert et al., 1991). These values are close to the pressure estimates of 10–11 kbar obtained by the *Grt–Ky–Pl–Qtz* barometer for kyanite–garnet gneisses of the Belomorian Group in the Kandalaksha Bay shore (Myskova, 2002). In other words, the prograde metamorphism of the Belomorian Complex corresponded to the high-pressure amphibolite facies.

The gabbro-norites (see Table 1 for their mineralogical composition) are massive rocks without traces of primary layering and with relics of an ophitic (Fig. 1a) and gabbro (Fig. 1b) texture. The primary magmatic minerals of these rocks are inverted pigeonite (sometimes with relict olivine in it) and pigeonite-augite, high-Ti biotite, and labradorite-bytownite plagioclase. The bulk-rock compositions of weakly altered gabbroids from the marginal part of the massif (Table 9) show variations from gabbro-norite to leucogabbro-norite. The contacts with the host rocks are sharp, without any traces of thermal aureoles. Conversely, the metagabbroids in direct contacts with the wall rocks, particularly where the latter bear abundant granite veins, are strongly amphibolized and transformed into apogabbro potassic feldspar-, biotite-, and quartz-bearing amphibolites with a newly formed lineation, which coincides with the gneissosity of the wall rocks.

The good preservation of the magmatic minerals of the gabbro-norites outside the marginal amphibolite zone offers the possibility of studying their chemistry. The inverted pigeonite-augite consists of a matrix of low-Na magnesian augite with X_{Fe} = 0.19–0.25 (Table 2) and orthopyroxene lamellae (Fig. 1c). The inverted pigeonite is composed of an orthopyroxene matrix (X_{Fe} = 0.32–0.40, Table 2) and augite lamellae. The biotite is relatively magnesian (X_{Fe} = 0.22–0.39) and very high in TiO_2 (5.2–6.7 wt %; Table 3). The composition of the plagioclase varies from labradorite to bytownite (50–80% *An*, Table 4). Many plagioclase grains are replaced by andesine or oligoclase in the margins, perhaps, during the metamorphic stage, either under the effect of sodic metasomatism or because of the incorporation of the anorthite end member during the formation of grossular–pyrope–almandine rims between plagioclase and orthopyroxene (Fig. 1b). In some metagabbro-norite samples, the cores of labradorite grains contain small prismatic inclusions of magmatic water-clear potassic feldspar with 28–30% of the albite end member (Table 5), a fact suggesting a very high crystallization temperature. The ore minerals are magnetite and titanomagnetite.

Traces of Svecofennian metamorphism are always discernible in the gabbro-norites, although the metamorphic alterations are merely embryonic. These alterations occur in the form of *Opx–Cpx–Grt* coronas between olivine and plagioclase, *Cpx–Grt* or *Grt* coronas between magmatic orthopyroxene and labradorite

[1] Abbreviations: *Ab*—albite, *Ac*—acmite, *An*—anorthite, *Anz*—andesine, *Ath*—anthophyllite, *Aug*—augite, *Bt*—biotite, *Btw*—bytownite, *Cal*—calcite, *Cpx*—clinopyroxene, *Ed*—edenite, *En*—enstatite, *Fs*—ferrosilite, *Fsp*—feldspar, *Grt*—garnet, *Hbl*—hornblende, *Jd*—jadeite, *Kfs*—potassic feldspar, *Ky*—kyanite, *Lbr*—labradorite, *Ma*—marialite, *Me*—meionite, *Olg*—oligoclase, *Opx*—orthopyroxene, *Pig*—pigeonite, *Pig-Aug*—pigeonite-augite, *Prg*—pargasite, *Px*—pyroxene, *Qtz*—quartz, *Scp*—scapolite, *Spl*—spinel, *Ts*—tschermakite, *Wol*—wollastonite, *Fl*—fluid, *Liq*—melt, X_{Fe}—total iron mole fraction [$Fe_{tot}/(Fe_{tot} + Mg)$], X_{H_2O}—water mole fraction, X^{Fl}_{NaCl}—NaCl mole fraction in fluid, a_{H_2O}—water activity, a_{Cl}—chlorine activity, *mag*—magmatic, *met*—metamorphic.

Table 1. Mineralogical compositions of the samples used in this research

Sample	Magmatic				Metamorphic											
	Pig	*Aug*	*Lbr*	*Bt*	*Cpx*	*Grt*	*Hbl*	*Ath*	*Opx*	*Bt*	*Anz*	*Olg*	*Scp*	*Cal*	*Kfs*	*Qtz*
Zone I: amphibolized metagabbro-norites with magmatic minerals and textures																
127a	+	±	+	+	–	–	±	–	±	±	+	–	–	–	–	–
27	+	+	+	+	+	+	±	–	±	–	+	–	–	–	–	–
25	+	+	+	+	+	+	±	–	–	±	+	–	–	–	–	–
24	+	+	+	+	±	+	±	+	±	±	+	–	–	–	–	–
19	+	±	+	+	±	+	±	±	–	±	+	–	–	–	–	–
18	+	+	+	+	–	+	+	–	–	±	+	–	–	–	–	–
Zone II: apogabbroic *Hbl–Pl* ± *Scp* ± *Qtz* plagioamphibolites with rare magmatic relics																
119B	+	+	+	+	–	–	+	+	±	±	+	–	–	–	–	–
118A	±	+	+	±	–	–	+	+	+	+	+	–	–	–	–	–
118	+	+	+	+	+	+	+	±	±	+	+	–	–	–	–	–
115B	+	–	–	+	–	–	+	+	±	+	+	–	–	–	–	–
16	–	+	±	±	±	+	+	–	–	+	+	±	±	–	–	–
15	–	±	–	±	–	–	+	–	–	+	+	+	+	±	–	–
14	–	±	±	±	–	–	+	–	–	+	+	+	+	+	–	+
6	–	–	–	±	–	–	+	±	–	+	+	+	+	–	–	+
Zone III: K-feldspathized *Hbl–Bt–Pl–Kfs* ± *Scp* ± *Qtz* apogabbroic amphibolites																
114	–	–	–	–	–	–	+	+	–	+	–	+	+	–	–	+
12	–	±	–	–	–	–	+	–	–	+	–	+	+	–	+	+
10	–	–	–	–	–	–	+	–	–	±	–	+	–	–	+	+
9	–	–	–	–	–	–	+	–	–	+	–	+	–	–	+	+
5	–	–	–	–	–	–	+	–	–	+	–	+	+	–	+	+
4	–	–	–	–	–	–	+	–	–	+	–	+	+	–	+	+
Zone IV: skialiths of *Hbl–Bt–Pl–Kfs* ± *Scp* ± *Qtz* amphibolites in gneiss-granites																
3b	–	–	–	–	–	–	+	–	–	+	–	+	+	–	+	+
3a	–	–	–	–	–	–	+	–	–	+	–	+	+	–	+	+
3	–	–	–	–	–	–	+	–	–	+	–	+	+	–	+	+
2	–	–	–	–	–	–	+	–	–	+	–	+	–	–	+	+
0	–	–	–	–	–	–	+	–	–	+	–	+	–	–	+	+
Gneiss-granites																
2a	–	–	–	–	–	–	±	–	–	+	–	+	–	–	+	+
1	–	–	–	–	–	–	±	–	–	+	–	+	–	–	+	+

(Fig. 1b), and *Grt–Cpx–Spl*, *Cpx–Spl*, and *Hbl–Spl* coronas between orthopyroxene and bytownite. The gabbroids without visible olivine, which occur in the contact zone with gneiss-granites, the corona-forming reactions are

$$Opx_{mag} + Lbr \pm H_2O \longrightarrow Grt + Cpx_{Ca} \pm Hbl + Olg, \quad (1)$$

$$Opx_{mag} + Btw \pm H_2O \longrightarrow Grt + Cpx_{Ca\text{-}Na} \pm Hbl + Olg + Spl. \quad (2)$$

The most ubiquitous and mineralogically diverse type of the coronas is, according to Larikova (2000) triple rims between olivine and plagioclase with the mineral succession $Ol_{mag} \longleftrightarrow Opx \longleftrightarrow Cpx_{Ca} \longleftrightarrow Grt \longleftrightarrow Pl_{mag}$. Along with clinopyroxene and garnet, orthopyroxene of the coronas is of metamorphic genesis, a fact proving the equilibrium crystallization of orthopyroxene during the metamorphism of the quartz-free gabbro-norites. The composition of the metamorphic orthopyroxene is close to that of the magmatic orthopyroxene and sometimes differs from it only in having a slightly elevated (up to 1.5–2.5 wt %) Al_2O_3 concentration and a somewhat higher X_{Fe}. The number of the rim types in the olivine-free norites decreases to two:

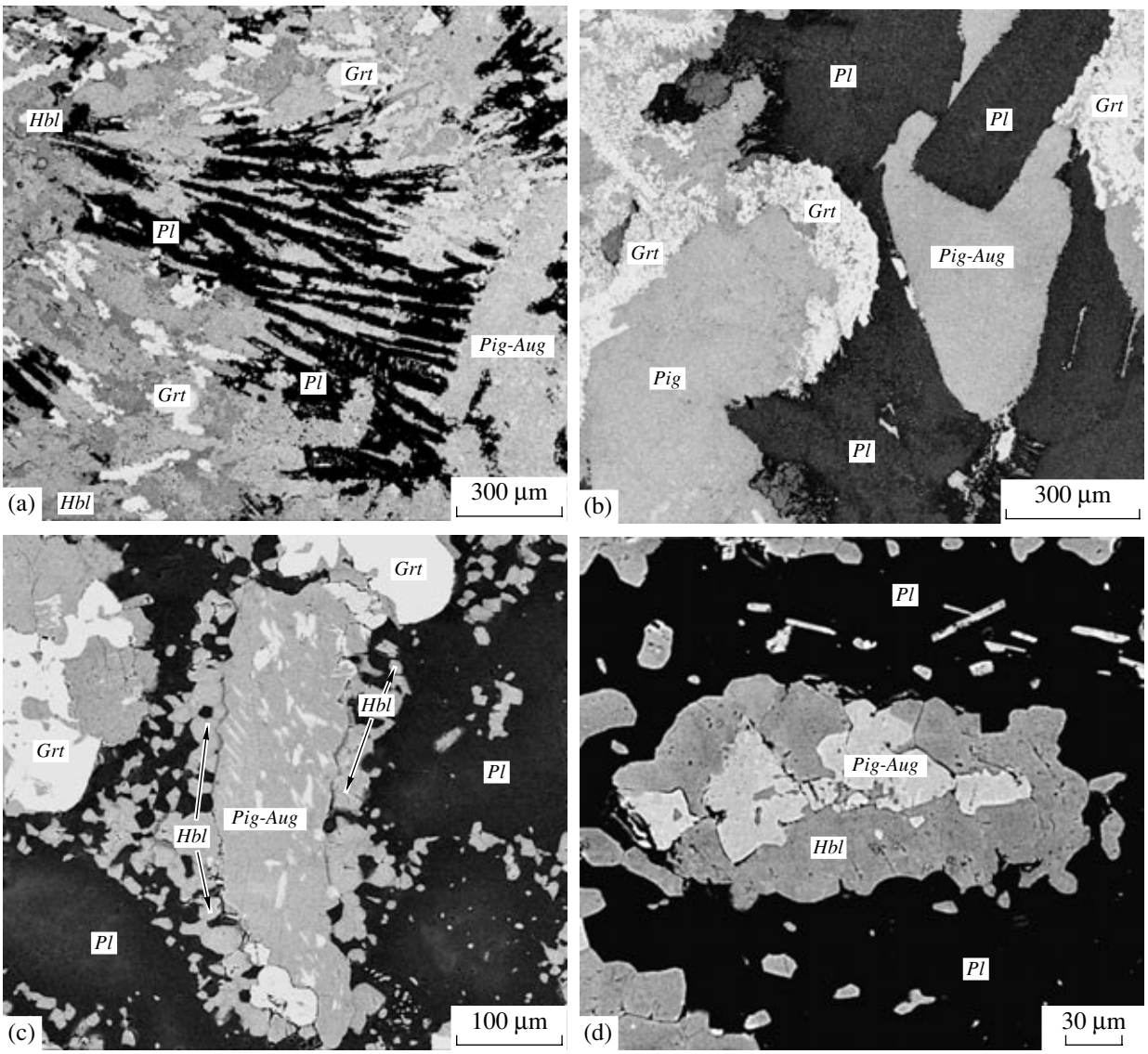

Fig. 1. Textures of metagabbro-norites in zones I and II (here and in Figs. 2, 3, and 9a, BSE images). (a) Relics of an ophitic texture. Magmatic pyroxenes and plagioclase are replaced by individual grains of hornblende and garnet that do not form coronitic textures. (b) Relics of a gabbro texture. Garnet corona rims develop only at contacts between pigeonite and labradorite and is absent from contacts between pigeonite-augite and plagioclase. (c) Embryonic *Hbl* ± *Anz* kelyphite rims around inverted pigeonite-augite (with *Opx* ingrowths) at contacts with *Lbr-Btw*; crystals at the bottom left are altered Pl_{mag} (An_{80} in cores and An_{38} in *Hbl–Pl* rims). (d) Pigeonite-augite relics in hornblende from amphibolized metagabbro-norite, zone II.

$Opx_{mag} \longleftrightarrow Cpx_{Ca} \longleftrightarrow Grt \longleftrightarrow Lbr_{mag}$, with *Cpx* replacing *Opx* and *Grt* replacing labradorite. Spinel-bearing rims develop when the $Opx(Ol) \longleftrightarrow Pl$ reaction is participated by a less silicic plagioclase bytownite instead of labradorite (Korikovsky, 2005). These rims sometimes contain no garnet but bear hornblende, so that the succession of the minerals is as follows: $Opx_{mag} \longleftrightarrow Cpx_{Ca\text{-}Na}(\pm Spl) \longleftrightarrow Hbl + Spl + Olg$ (after Btw_{mag}). In addition to coronitic textures, the gabbro contain individual garnet grains, patchy accumulations of newly formed hornblende around pyroxenes (Fig. 1a), and relatively low-Ti biotite in pseudomorphs after high-Ti magmatic biotite. The regional metamorphic transformations of gabbroids in the Belomorian series in the area of Kandalaksha Bay were beyond the scope of this publication, and their descriptions can be found in (Alekseev et al., 1999; Larikova, 2000). Here we present only a brief characterization of the chemistries of the metamorphic minerals of this massif in order to follow their further evolution during the contact–reaction transformations.

The garnet in reaction rims is characterized by broadly varying X_{Fe} (0.53–0.83) and pyrope concentrations (17–50%) at a relatively low concentration of grossular (11–20%). The weak zoning of garnet in the rims (an increase in the Ca concentration and a decrease

Table 2. Representative microprobe analyses (wt %) of inverted magmatic pigeonite-augite and pigeonite from the coronitic metagabbro-norites

Component	*Cpx* matrix of pigeonite-augite			*Opx* matrix of pigeonite		
	25*		16	25		118
SiO_2	52.85	52.8	51.65	52.21	53.26	54.06
TiO_2	0.30	0.07	0.18	0.04	–	0.16
Al_2O_3	2.43	1.54	2.09	1.02	0.96	1.23
FeO	5.9	6.81	7.65	25.25	21.15	17.49
MnO	0.34	0.10	0.19	0.18	0.2	0.31
MgO	13.82	14.52	12.88	20.88	24.12	25.84
CaO	23.48	23.47	23.3	0.26	0.2	0.35
Na_2O	0.85	0.68	0.79	0.12	0.11	–
K_2O	–	–	–	–	–	–
Total	99.87	99.94	98.73	99.97	99.98	99.41
	6O					
Si	1.95	1.95	1.94	1.96	1.96	1.97
Al(IV)	0.05	0.06	0.06	0.04	0.04	0.03
Al(VI)	0.06	0.01	0.03	0.01	–	0.02
Ti	0.01	–	0.01	–	–	–
Fe^{3+}	0.04	0.08	0.07	0.03	0.04	–
Fe^{2+}	0.14	0.12	0.17	0.76	0.61	0.53
Mn	0.01	–	0.01	0.01	0.01	0.01
Mg	0.76	0.80	0.72	1.17	1.32	1.41
Ca	0.93	0.93	0.94	0.01	0.01	0.01
Na	0.06	0.05	0.06	0.01	0.01	–
K	–	–	–	–	–	–
$X_{Fe\ tot}$	0.16	0.14	0.19	0.42	0.32	0.27
Jd	5.2	1.3	3.3			
Ac	0.9	3.5	2.4			
Ts_{tot}	4.5	5.2	5.5			
Wol	44.0	43.7	44.2			
En	37.9	39.9	36.0			
Fs	7.5	6.4	8.6			

Note: Ts_{tot} is the sum of the Ca–Fe, Ca–Ti, and Ca–Ts end members.
* Sample numbers here in tables below.

in the contents of Mg and Fe toward contacts with plagioclase) was controlled mostly by the kinetics of corona growth, although equant grains sometimes display discernible prograde growth zoning (Larikova, 2000). The garnets always contain small inclusions of clinopyroxene and hornblende, which allowed us to use them to evaluate the temperature of the corona-forming process. In double *Grt–Cpx* rims at *Opx–Lbr* contacts, metamorphic clinopyroxene composes monomineralic inner rim around orthopyroxene and occurs as small inclusions in the outer garnet rim around plagioclase. At *Opx–Btw* contacts, metamorphic *Cpx* most commonly develops as monomineralic or clinopyroxene–spinel rims. The compositions of the coronitic clinopyroxene itself notably differ in contact with labradorite and bytownite. The clinopyroxene is augite that contains 5–10% *Jd* in rims between *Opx* and *Lbr* and has a variable composition and is more sodic (up to omphacite) with 12–35% *Jd* in spinel-bearing rims between *Opx* and *Btw*. This unexpected difference is explained by the fact that, at given *P–T* parameters, the *Jd* solubility in *Cpx* drastically increases in silica-poor (spinel-bearing) domains (Korikovsky, 2005). The contact described above contains no omphacite–spinel–oligo-

Table 3. Representative microprobe analyses (wt %) of primary magmatic (from the gabbronorites) and metamorphic biotite in the rocks of zones I–IV

Component	Magmatic			From recrystallized metagabbro-norites										
				I	II			III			IV (skialiths and gneiss-granites)			
	127a		25	25	15		14	12	9	5	3b	3a	2	0	1
SiO_2	37.85	37.85	37.92	38.97	37.76	37.60	37.94	37.76	37.64	37.50	37.40	36.65	35.80	36.29	35.65
TiO_2	6.73	5.63	5.17	2.58	3.28	2.99	2.80	2.08	3.31	2.37	2.75	2.36	2.59	1.91	2.60
Al_2O_3	14.61	15.27	14.07	15.08	14.90	14.75	14.78	15.66	15.04	15.29	15.25	15.07	15.04	15.12	15.33
FeO	8.98	8.57	15.68	11.98	16.03	17.43	16.09	17.70	17.32	18.09	19.47	21.06	22.53	24.07	24.19
MnO	0.09	0.01	0.00	0.00	0.13	0.03	0.15	0.23	0.18	0.37	0.15	0.50	0.50	0.18	0.19
MgO	18.03	18.34	13.90	17.66	14.66	14.23	14.20	14.18	13.20	14.56	11.49	10.90	10.21	9.58	8.80
CaO	0.06	0.09	0.09	0.03	0.11	0.00	0.05	0.13	0.00	0.04	0.10	0.00	0.16	0.11	0.00
Na_2O	0.30	0.32	0.22	0.00	0.16	0.02	0.18	0.30	0.00	0.06	0.10	0.11	0.02	0.33	0.15
K_2O	9.78	10.22	9.59	9.96	9.12	9.17	9.99	9.01	9.83	7.68	9.97	9.35	9.27	9.33	9.66
Cl	0.08	0.01	0.17	0.15	0.35	0.38	0.31	0.16	0.28	0.14	0.21	0.30	0.28	0.17	0.22
Total	96.50	96.30	96.80	96.40	96.50	96.60	96.50	97.20	96.80	96.10	96.90	96.30	96.40	97.10	96.80
	11O														
Si	2.81	2.80	2.89	2.89	2.87	2.87	2.88	2.84	2.88	2.87	2.88	2.86	2.81	2.83	2.80
Al(IV)	1.19	1.20	1.11	1.11	1.13	1.13	1.12	1.16	1.12	1.13	1.12	1.14	1.19	1.17	1.20
Al(VI)	0.09	0.13	0.16	0.21	0.21	0.20	0.20	0.23	0.23	0.25	0.26	0.24	0.20	0.21	0.22
Ti	0.38	0.31	0.30	0.14	0.19	0.17	0.16	0.12	0.19	0.14	0.16	0.14	0.15	0.11	0.15
Fe	0.56	0.53	1.00	0.74	1.02	1.11	1.02	1.11	1.11	1.16	1.25	1.37	1.48	1.56	1.59
Mn	0.01	0.00	0.00	0.00	0.01	0.00	0.01	0.01	0.01	0.02	0.01	0.03	0.03	0.01	0.01
Mg	2.00	2.02	1.58	1.95	1.66	1.62	1.60	1.59	1.50	1.66	1.32	1.27	1.19	1.11	1.03
Ca	0.00	0.01	0.01	0.00	0.01	0.00	0.00	0.01	0.00	0.00	0.01	0.00	0.01	0.01	0.00
Na	0.04	0.05	0.03	0.00	0.02	0.00	0.03	0.04	0.00	0.01	0.02	0.02	0.00	0.05	0.02
K	0.93	0.96	0.93	0.94	0.88	0.89	0.97	0.87	0.96	0.75	0.98	0.93	0.93	0.93	0.97
Cl	0.01	0.01	0.02	0.02	0.04	0.08	0.04	0.02	0.04	0.02	0.05	0.04	0.04	0.02	0.03
$X_{Fe\ tot}$	0.22	0.21	0.39	0.28	0.38	0.41	0.39	0.41	0.43	0.41	0.49	0.52	0.55	0.58	0.61

clase–hornblende coronites, but they were found at a distance of 20–30 m from the contact. The metamorphic hornblende contained in the corona and rock matrix (Fig. 1a) is magnesian pargasite or edenite.

The *Grt–Cpx* and *Grt–Hbl* thermometry of coronitic rims in the metagabbro-norites with the use of *Cpx* and *Hbl* inclusions in *Grt* (Powell, 1985; Perchuk, 1989) yields their peak temperatures of 620–670°C (Korikovsky, 2005), which practically coincides with the estimates for the host *Grt–Cpx–Hbl–Pl* amphibolites and confirms genetic links between their metamorphism. However, it is impossible to apply the *Grt–Hbl–Pl–Qtz* or *Grt–Cpx–Pl–Qtz* barometers to these metagabbroids because they are, in contrast to the amphibolites, quartz-free rocks. Because of this, we assumed that the pressure during the coronitization of the gabbroids was the same as during the metamorphism of the amphibolites, i.e., 9-10 kbar. This assumption is indirectly supported by the fact that these are the minimum pressure values under which omphacite can crystallize in silica-undersaturated coronites. Inasmuch as gneiss-granites and migmatites in the Belomorian Complex and the related contact–metamorphic processes are obviously synmetamorphic, the following parameters can be assumed for the metasomatic recrystallization and granitization of the metagabbro-norites: ***T* = 660–700°C, *P* = 9.5–10.5 kbar.**

GNEISS-GRANITES AND THEIR EFFECT ON METAGABBRO-NORITES

Metagabbro-norites in contact with gneisses and amphibolites devoid of granite veins are almost not affected by metasomatic alterations but are altered very strongly in contact with gneiss-granites. Small gneiss-granite bodies are part of a diverse vein complex that occurs in the surrounding supracrustal rocks and comprises two genetic types. The injection granite veins

Table 4. Representative microprobe analyses (wt %) of partly recrystallized magmatic and newly formed metamorphic plagioclase in the rocks of zones I–IV

Component	I								II				III		IV	
	25								16		15		12	4	1	0
	Recrystallized magmatic *Pl*					From *Hbl–Pl* kelyphite around pigeonite (pigeonite-augite)			From the matrix of apogabbroic amphibolites						From the matrix of skialiths and gneiss-granites	
	c*	i	m	c	m											
SiO_2	47.67	57.35	58.96	53.58	58.38	59.37	58.28	59.16	60.15	59.48	61.89	62.8	61.67	61.67	62.55	62.67
Al_2O_3	33.00	26.79	25.59	29.30	25.86	25.29	25.88	25.19	24.68	24.81	24.16	22.83	23.34	23.62	23.03	0.05
FeO	0.00	0.00	0.04	0.10	0.39	0.21	0.37	0.30	0.12	0.44	0.17	0.22	0.16	0.02	0.3	23.01
CaO	16.84	9.48	8.09	12.79	8.27	7.90	8.09	7.61	6.91	7.52	5.34	5.07	5.5	5.52	4.67	0.14
Na_2O	2.23	6.07	7.00	4.08	6.78	6.79	7.07	7.39	7.92	7.47	8.35	8.65	8.97	8.87	9.28	4.42
K_2O	0.09	0.20	0.22	0.15	0.21	0.25	0.23	0.18	0.08	0.06	0.00	0.05	0.13	0.05	0.07	9.41
Total	99.94	99.97	99.96	99.94	99.96	99.97	99.95	99.93	99.60	99.45	99.97	99.91	99.77	99.75	99.90	99.85
	8O															
Si	2.18	2.58	2.64	2.44	2.62	2.66	2.61	2.64	2.68	2.66	2.75	2.79	2.74	2.74	2.77	2.77
Al(IV)	1.78	1.42	1.35	1.57	1.37	1.34	1.36	1.33	1.30	1.31	1.27	1.20	1.22	1.24	1.20	1.20
Fe	0.00	0.00	0.00	0.00	0.01	0.01	0.01	0.01	0.00	0.02	0.01	0.01	0.01	0.00	0.01	0.01
Ca	0.83	0.46	0.39	0.62	0.40	0.38	0.39	0.36	0.33	0.36	0.25	0.24	0.26	0.26	0.22	0.21
Na	0.20	0.53	0.61	0.36	0.59	0.59	0.61	0.64	0.68	0.65	0.72	0.75	0.77	0.76	0.80	0.81
K	0.01	0.01	0.01	0.01	0.01	0.01	0.01	0.01	0.00	0.00	0.00	0.00	0.01	0.00	0.00	0.01
An, %	80 → 46 → 38			63 → 40		39	38	36	32	36	26	24	25	26	22	20

Note: Grain parts: c—core, i—intermediate zone(s), m—margin.

Table 5. Representative microprobe analyses (wt %) of magmatic potassic feldspar in gabbro-norite and this mineral in apogabbroic amphibolites, skialiths, and gneiss-granites the of zones III–IV

Component	Gabbro with Kfs_{mag}	Amphibolites with *Kfs*		Skialiths and gneiss-granites		
		III		IV		
	25	9	5	1	2	0
SiO_2	53.99	64.69	64.53	64.86	63.37	64.53
Al_2O_3	33.37	17.85	18.24	18.49	18.16	18.39
FeO	0.32	0.11	0.05	–	–	0.04
CaO	0.69	0.07	0.03	–	–	–
Na_2O	2.42	0.09	1.27	0.65	0.58	0.41
K_2O	8.86	17.09	15.11	15.86	15.79	16.18
Total	99.65	99.90	99.23	99.86	97.90	99.55
	8O					
Si	2.45	3.00	2.99	3.00	2.99	3.00
Al(IV)	1.78	0.98	1.00	1.01	1.01	1.01
Fe	0.01	–	–	–	–	–
Ca	0.03	–	–	–	–	–
Na	0.21	0.01	0.11	0.06	0.05	0.04
K	0.51	1.01	0.89	0.94	0.95	0.96
Ab, %	28	1	11	6	5	4

Table 6. Representative microprobe analyses (wt %) of hornblende in recrystallized metagabbroids, skialiths, and gneiss-granites the of zones I–IV

Component	I			II				III				IV			
												Skialiths			Granite
	25			16	15		14	12	9	4		3a		0	1
SiO_2	45.81	44.15	43.57	45.77	45.34	43.55	42.66	43.00	42.43	41.50	41.54	39.74	39.27	38.95	40.08
TiO_2	0.74	0.78	1.16	1.07	0.95	1.01	1.13	0.92	1.16	0.97	0.79	1.19	1.07	0.78	0.84
Al_2O_3	12.38	13.27	12.85	9.85	9.89	11.80	11.84	11.07	11.15	11.61	11.26	11.87	11.97	12.13	12.36
FeO	11.00	11.47	11.91	13.43	14.40	15.20	15.56	16.71	17.42	18.99	19.12	23.11	23.29	24.77	23.40
MnO	0.00	0.06	0.13	0.00	0.13	0.23	0.30	0.35	0.33	0.21	0.26	0.34	0.36	0.39	0.32
MgO	13.45	12.98	12.83	13.15	12.19	11.61	10.76	10.63	10.04	9.31	8.86	6.92	6.32	6.16	6.42
CaO	12.73	12.43	12.63	12.50	12.40	12.00	11.94	12.77	12.52	11.82	12.32	11.36	11.88	11.58	11.12
Na_2O	0.98	1.33	1.22	1.21	1.36	1.45	1.55	1.27	1.44	1.34	1.50	1.45	1.35	1.40	1.40
K_2O	1.12	1.37	1.45	0.89	0.90	1.22	1.33	1.37	1.47	1.77	1.45	1.78	1.79	1.73	1.67
Cl	0.15	0.19	0.07	0.06	0.25	0.41	0.44	0.16	0.41	0.37	0.29	0.33	0.39	0.14	0.19
Total	98.36	98.03	97.82	97.93	97.76	98.48	95.50	98.25	98.30	97.89	97.40	98.10	97.70	98.03	97.80
	23O														
Si	6.61	6.44	6.37	6.86	6.72	6.45	6.42	6.48	6.41	6.35	6.41	6.20	6.20	6.14	6.19
Al(IV)	1.39	1.56	1.63	1.14	1.28	1.55	1.58	1.52	1.59	1.65	1.59	1.80	1.80	1.86	1.81
Al(VI)	0.72	0.72	0.58	0.60	0.44	0.51	0.52	0.45	0.46	0.44	0.46	0.38	0.43	0.39	0.45
Ti	0.08	0.09	0.13	0.12	0.11	0.11	0.13	0.10	0.11	0.11	0.09	0.14	0.13	0.09	0.08
Fe^{3+}	0.06	0.10	0.18	0.17	0.09	0.25	0.17	0.12	0.17	0.28	0.13	0.41	0.28	0.48	0.36
Fe^{2+}	1.27	1.30	1.39	1.07	1.69	1.63	1.79	1.99	2.08	2.15	2.33	2.60	2.79	2.78	2.83
Mn	0.00	0.00	0.01	0.00	0.01	0.01	0.02	0.02	0.02	0.01	0.02	0.02	0.02	0.03	0.03
Mg	2.89	2.82	2.79	2.94	2.69	2.56	2.41	2.39	2.25	2.12	2.04	1.61	1.49	1.45	1.40
Ca	1.97	1.94	1.98	2.01	1.97	1.90	1.92	2.06	2.02	1.94	2.04	1.90	2.01	1.96	1.98
Na	0.28	0.38	0.35	0.35	0.39	0.42	0.45	0.37	0.40	0.40	0.45	0.44	0.41	0.43	0.28
K	0.21	0.26	0.27	0.17	0.17	0.23	0.26	0.26	0.30	0.35	0.29	0.35	0.36	0.35	0.34
Cl	0.04	0.05	0.02	0.01	0.07	0.11	0.12	0.04	0.11	0.10	0.08	0.09	0.11	0.04	0.06
$X_{Fe\ tot}$	0.31	0.33	0.34	0.37	0.40	0.42	0.45	0.47	0.50	0.53	0.55	0.65	0.67	0.69	0.69
$(Na + K)_A$	0.46	0.60	0.60	0.52	0.54	0.59	0.66	0.63	0.70	0.70	0.74	0.73	0.77	0.73	0.78
Na_B	0.02	0.03	0.02	0.00	0.02	0.05	0.04	0.00	0.00	0.04	0.00	0.06	0.01	0.04	0.02
Hbl type	*Mg-Hbl*	*Prg*	*Prg*	*Ed*	*Ed*	*Prg*	*Prg*	*Prg*	*Prg*	Fe-*Prg*	Fe-*Prg*	Fe-*Prg*	Fe-*Prg*	Fe-*Prg*	Fe-*Prg*

have sharp, sometime cutting contacts and pegmatoid textures and are usually not accompanied by discernible wall-rock alterations. The anatectoid gneiss-granites have a subparallel gneissose structure and do not have sharp contacts with the host amphibolites and gneisses, showing obvious evidence that their in-situ melting and crystallization proceeded under the effect of inflowing silicic–alkaline fluids. This follows from (i) the occurrence of variably dissolved and debasified host-rock skialiths in the gneiss-granites; (ii) aureoles of metasomatic feldspathization and biotitization of the host rocks, with the thicknesses of these aureoles often much greater than the thicknesses of the veins themselves; and (iii) the "diffuse" contours of the gneiss-granite veins with traces of their expansion and the replacement of the surrounding amphibolites. The latter feature is atypical of leucosomes derived in closed systems and having "passive" contacts with more basic rocks from which they are derived.

The gneiss-granite vein in contact with the metagabbro-norite belongs to the second type. It is 3–4 m thick, and its aureole of metasomatic alterations in the metagabbroids is more than 15 m thick. The gneiss-granites have a *Bt* ± *Hbl–Kfs–Pl–Qtz* composition, gneissose texture, and contain numerous elongated large (0.1–0.5 m) and small (0.2–5.0 cm) skialiths of apogabbro amphib-

Table 7. Representative microprobe analyses (wt %) of anthophyllite and coexisting metamorphic orthopyroxene in amphibolized metagabbro-norites of zone II

Component	115B		119B		118A
	Ath		*Ath*	*Opx*	
SiO_2	55.69	56.13	56.31	53.17	53.21
TiO_2	–	0.02	0.02	0.11	0.05
Al_2O_3	0.70	0.48	0.79	2.17	1.27
FeO	18.72	17.63	15.06	17.32	19.58
MnO	0.62	0.47	0.37	0.24	0.24
MgO	21.54	22.13	24.61	25.64	25.14
CaO	0.75	0.70	0.36	0.99	0.25
Na_2O	0.09	–	0.21	–	–
K_2O	–	0.04	0.06	–	–
Total	98.11	97.60	97.80	99.64	99.74
			23O		
Si	7.91	7.97	7.85	1.94	1.96
Al(IV)	0.09	0.03	0.14	0.06	0.04
Al(VI)	0.03	0.05	–	0.03	0.02
Ti	–	–	–	–	–
Fe^{3+}	0.05	–	0.24	–	–
Fe^{2+}	2.17	2.09	1.51	0.53	0.60
Mn	0.07	0.06	0.04	0.01	0.01
Mg	4.56	4.68	5.11	1.39	1.38
Ca	0.11	0.11	0.05	0.04	0.01
Na	0.02	–	0.06	–	–
K	–	0.01	0.01	–	–
$X_{Fe\ tot}$	0.33	0.31	0.25	0.27	0.30

olites, which are transformed into thin mesocratic *Bt–Hbl–Fsp–Qtz* bans of black color clearly differ from the host pinkish granite. The amount of skialiths increases closer to metagabbro. The contact between the gneiss-granite and metagabbro is sharp, and it can be clearly seen in exposures that *Bt–Hbl* skialiths in the gneiss-granite are fragments of metagabbro completely amphibolized and biotitized.

The examination of contact–reaction alterations zones in the metagabbro-norite allowed us to reveal that these alterations were induced by silicic–alkaline fluids expelled from the granite, and the intensity of recrystallization decreases away from the contact with granite. According to chemical analyses of the rocks (Tables 9, 10), these alterations result in the enrichment of the metagabbroids in silica and alkalis (K and Na) and in an increase in the X_{Fe} = Fe/(Fe + Mg) of these rocks and their Al/(Mg + Fe + Ca) ratio at a simultaneous decrease in the concentrations of Fe, Mg, and Ca. This process is pronounced mineralogically in an increase in the intensity of amphibolization, biotitization, feldspathization, scapolitization, and silification of the metagabbroids closer to the contact and the corresponding replacement of both magmatic (pigeonite, pigeonite-augite, labradorite-bytownite) and metamorphic (garnet and coronitic orthopyroxene and clinopyroxene) mafic minerals by feldspars and quartz. According to the change in the mineral assemblages, the aureole can be subdivided into the following four grades (zones): (I) very weakly amphibolized coronitic metagabbro-norites with relict magmatic minerals and textures; (II) apogabbroic *Hbl–Pl* ± Scp ± *Qtz* plagioamphibolite with rare magmatic relics; (III) K-feldspathized *Hbl–Bt–Pl–Kfs* ± *Scp–Qtz* apogabbroic amphibolites; (IV) *Bt* ± *Hbl–Kfs–Pl–Qtz* gneiss-granites with skialiths of bleached *Bt–Hbl–Pl–Kfs* ± *Scp–Qtz* amphibolites. Below we consider the composition of each of these zones and the corresponding reaction transformations.

Zone I: Very Weakly Amphibolized Coronitic Metagabbro-Norites

The first, the most distant from the gneiss-granite part of the metasomatic aureole (zone I) is characterized only by weak amphibolization of pyroxenes and andesinization of calcic plagioclase. The magmatic inverted pigeonite and pigeonite-augite are surrounded by thin rims (Fig. 1c) of minute grains of magnesian pargasite (X_{Fe} = 0.31–0.34, Table 6) in symplectite-like aggregates with andesine (36–39% *An*; Table 4). The high-Ti biotite is replaced (in margins) by pale metamorphic biotite that contains roughly twice less TiO_2 (Table 3). The rocks occasionally contain initial anthophyllite rims around pigeonite (anthophyllite is spread more widely in zone II, see below). Grains of magmatic labradorite and bytownite (63–80% *An*) are replaced by andesine (38–40% *An*) in margins, with a gradual decrease in the anorthite concentrations from the cores to margins of the plagioclase grains (Table 4).

The Cl concentrations in the mafic minerals are very low: 0.07–0.19 wt % in the amphiboles and 0.15 wt % in the biotite.

During the initial stage of the metamorphic alterations of the metagabbro-norites, their original ophitic, gabbroic, or apogabbroic coronitic textures remain well preserved (Figs. 1a, 1b). Judging from the development of two Na-bearing phases (hornblende and andesine) at contacts of orthopyroxene (clinopyroxene) with labradorite (bytownite), the replacement forefront was characterized by a slight inflow of Na and Si and a weak leaching of Ca. The summarizing reaction for zone I is

$$Opx + Cpx + Lbr\text{-}Btw + Na_2O \pm SiO_2 + H_2O \longrightarrow Hbl + Anz \pm CaO\uparrow. \quad (3)$$

The X_{Fe} of the newly formed hornblende (0.31–0.34) is intermediate between these values of the replaced magmatic pigeonite-augite and augite (Table 2), and it is thus reasonable to believe that this

Table 8. Representative microprobe analyses (wt %) of coexisting plagioclase and scapolite in amphibolized metabasites of zones II–IV

Component	II								III						IV	
	15				14				114		5		4		3b	
	Scp	*Pl*	*Scp*	*Pl*	*Scp*	*Pl*	*Scp*	*Pl*	*Scp*	*Pl*	*Scp*	*Pl*	*Scp*	*Pl*	*Scp*	*Pl*
SiO_2	53.64	61.89	54.68	62.80	52.26	61.32	54.45	61.92	56.24	63.76	53.29	61.75	51.08	61.89	50.84	61.54
Al_2O_3	25.16	24.16	23.97	22.83	25.24	3.69	23.83	23.19	23.34	22.76	24.53	24.01	25.20	23.79	24.78	23.79
FeO	–	0.17	0.66	0.22	0.04	0.25	0.16	0.18	0.08	–	–	–	0.03	0.10	0.05	0.03
CaO	12.23	5.34	10.24	5.07	13.11	5.90	9.90	5.06	8.53	4.37	11.79	5.41	14.28	5.48	13.07	5.81
Na_2O	7.17	8.35	7.96	8.65	6.66	8.71	8.34	9.14	8.65	8.90	7.71	8.66	6.16	8.51	7.00	8.48
K_2O	0.22	–	0.39	–	0.37	–	0.56	0.06	0.50	0.11	0.57	–	0.46	–	0.38	–
Cl	1.19	–	1.90	–	1.40	–	2.33	–	2.49	–	1.89	–	1.13	–	1.51	–
SO_3	0.18	–	–	–	0.83	–	0.12	–	–	–	–	–	1.51	–	0.08	–
Total	99.79	99.91	99.80	99.57	99.91	99.87	99.69	99.61	99.83	99.90	99.78	99.83	99.85	99.77	97.71	99.65
	Normalized to 16 cations for *Scp* and 8 O for *Pl*															
Si	7.73	2.75	7.91	2.79	7.65	2.72	7.92	2.75	8.06	2.83	7.78	2.74	7.59	2.75	7.62	2.73
Al(IV)	4.27	1.27	4.09	1.20	4.35	1.24	4.08	1.21	3.94	1.19	4.22	1.25	4.41	1.24	4.38	1.25
Fe	–	0.01	0.08	0.01	0.01	0.01	0.02	0.01	–	–	–	–	–	–	0.01	–
Ca	1.89	0.25	1.59	0.24	2.06	0.28	1.54	0.24	1.31	0.21	1.84	0.26	2.27	0.26	2.10	0.28
Na	2.00	0.72	2.23	0.75	1.89	0.75	2.35	0.79	2.40	0.77	2.18	0.74	1.77	0.73	2.04	0.73
K	0.04	–	0.07	–	0.07	–	0.10	–	0.09	–	0.11	–	0.09	–	0.07	–
Cl	0.29	–	0.46	–	0.35	–	0.57	–	0.60	–	0.46	–	0.28	–	0.38	–
SO_4	–	–	–	–	0.09	–	0.01	–	0	–	–	–	0.17	–	0.01	–
An, %		26		24		27		23		21		25		26		27
Me, %	49		42		52		40		35		46		47		51	

value is inherited in zone I from the magmatic pyroxenes.

Zone II: Apogabbroic Hbl–Pl ± Scp ± Qtz Plagioamphibolites with Rare Magmatic Relics

The amphibolization of the metagabbro-norite drastically intensifies closer to the contact with gneiss-granite. Magmatic pigeonite, pigeonite-augite and corona clinopyroxene are extensively replaced by an aggregate of edenitic or pargasitic hornblende and are preserved in this aggregate only as relics (Fig. 1d), completely disappearing near the inner boundary of zone II. The coronitic garnet is also replaced by hornblende (Fig. 2a) and is completely decomposed together with the pyroxenes. The pigeonite is replaced not only by Ca-amphibole but also by anthophyllite (Fig. 2a) and metamorphic orthopyroxene. The latter is the recrystallization product of magmatic pigeonite and sometimes contain 1–1.5 wt % more Al_2O_3 (compare Tables 2 and 7) and is devoid of augite lamellae but bear newly formed ingrowths of hornblende (Fig. 9a). The outer rims of this metamorphic orthopyroxene often develop around large pigeonite crystals during corona-forming reactions. In spite of the predominantly reaction relations in the *Opx–Ath* pair, some thin sections of rocks from zone II (only in quartz-free varieties) show the equilibrium coexistence of metamorphic orthopyroxene and newly formed anthophyllite, without any traces of replacements (Fig. 9a). The anthophyllite has an X_{Fe} = 25–33% (Table 7), which is roughly equal to the X_{Fe} of the magmatic pigeonite and confirms the origin of the anthophyllite at the expense of pigeonite. In coexisting *Ath–Opx* pairs, the latter is 2–3% more ferrous than the former (Table 7).

The gabbro-ophitic or coronitic texture of the metabasites is transformed into a metamorphic nematogranoblastic texture, in which amphibole aggregates often inherit their rounded morphologies from the primary pyroxenes. The X_{Fe} of the hornblende increases during amphibolization from 0.37 to 0.45 (Table 6), although this increase can be partially explained by the slightly elevated original X_{Fe} of the gabbroids (Table 9) but not by preferential Mg depletion, as is the case with the next zones. The rocks contain, along with the predominant hornblendes, newly formed blade-shaped flakes of metamorphic biotite (X_{Fe} = 0.38–0.41, 2.8–3.3 wt %

Table 9. Major- (wt %) and trace-element (ppm) composition of metasomatically weakly altered metagabbro-norites from zones I and II depending on their distance from the contact with gneiss-granite

Component	Metagabbro-norites with well preserved magmatic relics (zone I)					Apogabbroic *Pl* amphibolites with minor amounts of magmatic relics (zone II)			
	lgn	lgn	gn	gn	gn				
	27	24	19	17	25	16	15	14	6
	→ toward contact with gneiss-granite								
SiO_2	53.82	54.32	52.93	52.77	52.43	52.59	52.35	53.29	51.44
TiO_2	1.11	1.09	0.83	0.82	0.78	0.81	0.76	0.78	0.80
Al_2O_3	14.80	13.13	12.22	11.39	11.76	12.11	11.02	10.98	11.61
Fe_2O_3	1.94	2.56	2.87	3.33	3.12	2.58	4.53	4.41	2.65
FeO	8.57	7.90	7.30	7.38	7.87	8.51	6.77	7.18	9.85
MnO	0.15	0.15	0.15	0.16	0.17	0.17	0.17	0.17	0.17
MgO	5.21	5.76	6.83	8.04	7.95	7.67	8.62	8.11	7.10
CaO	9.03	8.47	9.65	9.05	9.69	9.73	9.17	9.53	9.80
Na_2O	2.58	2.57	2.11	1.97	2.15	2.31	1.74	1.63	1.89
K_2O	1.51	1.50	1.24	1.20	1.14	1.20	1.32	1.25	1.23
P_2O_5	0.12	0.15	0.10	0.10	0.08	0.09	0.08	0.08	0.08
S	0.04	0.05	0.06	0.04	0.04	0.04	0.05	0.05	0.05
LOI	1.64	1.78	2.96	2.72	2.26	1.57	2.69	2.09	2.37
Total	100.52	99.43	99.25	98.96	99.44	99.38	99.27	99.55	99.05
Cr	111	196	572	610	632	546	675	597	435
V	204	184	181	175	176	182	196	186	138
Co	41	49	54	48	55	52	58	46	39
Ni	92	91	160	159	156	149	177	149	82
Zn	92	84	86	95	92	93	172	106	117
Zr	124	136	97	102	93	100	97	91	137
Ba	430	489	385	359	326	342	330	257	697
Cl	229	287	199	263	202	240	1612	1892	1064
Fe/(Fe + Mg)	0.53	0.50	0.45	0.42	0.43	0.44	0.42	0.44	0.49
Na + K, at. un.	116	116	94	90	93	100	82	78	88
Mg + Fe + Ca, at. un.	434	437	474	507	518	512	525	522	522
Al/(Mg + Fe + Ca)	0.40	0.37	0.33	0.31	0.31	0.32	0.29	0.29	0.30
Al, at. un.	290	256	237	224	231	236	216	212	228

Note: The systematics of gabbroids is given according to the recalculated modal compositions of the least altered rocks: lgn—leucogabbro-norite, gn—gabbro-norite (Barker, 1979; Debon and Le Fort, 1983).

TiO_2; Table 3), which cut across hornblende grains (Fig. 2b).

In the front part of zone II, the remaining magmatic labradorite and bytownite are replaced first by andesine (32–36% *An*, sample 16, Table 4) and then, in the middle part of the zone, by oligoclase (24–26% *An*, sample 15, Table 4). This zone is the first to contain minor amounts of small quartz grains.

This reaction aureole is noted for the fact that it contains, starting in zone II, metasomatic scapolite and, in places, calcite, along with sodic plagioclase and hornblende. Scapolite is unevenly distributed in the rocks, and its contents vary from 0 to 10%. Initially, the scapolite (35–45% of the meionite end member, Table 8) composes (alone or together with calcite) thin veinlets cutting hornblende and oligoclase grains (Fig. 2c) or fills the interstitial space. Closer to the contact, they

Table 10. Major- (wt %) and trace-element (ppm) composition of metasomatically most strongly altered metagabbro-amphibolites, skialiths, and gneiss-granites from granitization zone

Component	K-feldspathized and biotitized apogabbroic amphibolites (zone III)				Gneiss-granites with skialiths of feldspathized and silicified apogabbroic amphibolites (zone IV)						
	→ toward contact with granite				amphibolite skialiths →					gneiss-granite	
	12	10	5	4	3b	3	3a	0	2	2a	1
SiO_2	53.17	54.87	56.12	55.20	56.34	65.30	65.94	67.56	67.22	68.52	69.08
TiO_2	0.83	0.65	0.66	0.78	0.71	0.58	0.58	0.50	0.55	0.42	0.43
Al_2O_3	12.58	12.67	13.37	12.38	13.77	14.28	14.98	14.45	14.41	14.60	14.96
Fe_2O_3	4.42	4.45	4.67	3.43	4.78	2.40	2.19	2.53	2.35	1.51	1.51
FeO	6.70	5.10	5.13	7.33	4.80	3.76	3.23	2.44	2.70	2.70	2.60
MnO	0.16	0.14	0.14	0.15	0.13	0.07	0.09	0.06	0.07	0.06	0.05
MgO	6.85	5.05	5.27	5.85	5.07	2.21	1.54	1.11	1.29	1.08	1.17
CaO	9.72	9.11	8.07	9.10	7.94	4.77	4.26	4.17	3.79	3.55	3.14
Na_2O	2.19	2.23	2.55	2.34	2.55	3.08	3.72	3.20	3.23	3.74	3.77
K_2O	1.35	2.15	1.79	1.67	2.26	1.98	1.97	3.31	3.14	2.06	2.61
P_2O_5	0.10	0.12	0.09	0.11	0.09	0.10	0.10	0.12	0.15	0.08	0.10
S	0.05	0.04	0.03	0.03	0.07	0.06	0.10	0.05	0.08	0.06	0.15
LOI	1.52	3.80	1.78	0.78	2.31	1.86	1.96	1.14	1.68	1.78	0.98
Total	99.64	100.38	99.57	99.15	100.81	100.44	100.65	100.64	100.67	100.17	100.56
Cr	349	435	210	312	181	73	35	23	28	22	24
V	176	138	154	184	148	106	61	58	63	53	48
Co	47	39	32	38	34	23	16	9	12	6	9
Ni	103	82	66	85	81	40	25	15	21	18	21
Zn	108	117	124	135	114	77	68	90	68	61	60
Zr	100	137	123	107	121	152	172	230	298	162	224
Ba	184	697	455	317	666	845	568	899	909	663	699
Cl	2261	1064	1362	1466	1687	653	503	300	412	419	356
Fe/(Fe + Mg)	0.47	0.50	0.49	0.50	0.50	0.60	0.65	0.50	0.68	0.67	0.65
Na + K, at. un.	99	115	120	109	130	142	162	174	170	163	178
Mg + Fe + Ca, at. un.	492	414	404	449	396	224	186	205	167	147	138
Al/(Mg + Fe + Ca)	0.50	0.60	0.65	0.54	0.68	1.25	1.58	1.39	1.69	1.95	2.12
Al, at. un.	248	249	261	241	269	280	294	284	282	286	293

give way to rounded euhedral grains of scapolite in equilibrium with newly formed plagioclase and hornblende (Fig. 2d). The calcite formed concurrently with the scapolite also forms individual grains equilibrated with hornblende, scapolite, and *Pl* (Fig. 3a).

An increase in the Cl concentration in the fluids of zone II was the reason for the notable increase in the Cl contents in the amphiboles (up to 0.44 wt %) and biotite (up to 0.38 wt %) (Tables 3 and 6).

According to mineralogical transformations, zone II is characterized by the introduction of Na (amphibolization of its pyroxenes and oligoclasization of the andesine), weak inflow of K (biotitization), and very significant addition of Cl and CO_2 (scapolitization and the sporadic development of calcite) at an insignificant removal of Ca (replacement of the pigeonite-augite). Because of this, the summarizing reaction for zone II has the form

$$Opx(Cpx) + Lbr(Anz) \pm Grt + Na_2O \pm K_2O \pm SiO_2 + H_2O + Cl + CO_2 \longrightarrow Hbl_{>Cl} + Bt \pm Ath + Olg + Scp \pm Cal + CaO\uparrow. \quad (4)$$

As a result, the *Opx*, *Cpx*, and *Grt* of zone II are replaced by hornblende and biotite with a sporadic admixture of anthophyllite. The plagioclase becomes even more sodic, and the weakly amphibolized coronitic and non-coronitic metagabbro-norites are trans-

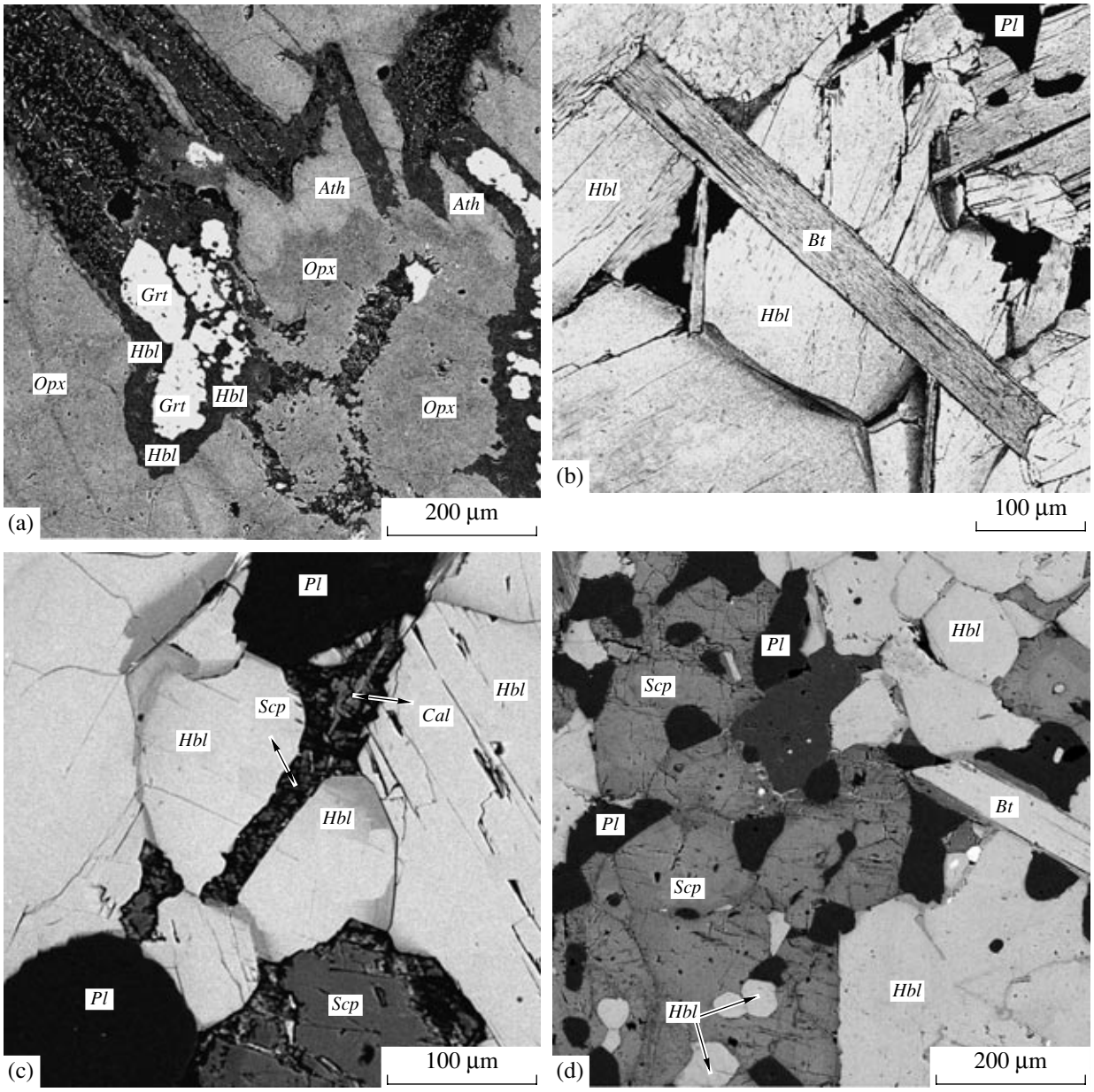

Fig. 2. Metagabbro-norites in zones II and III. (a) Metamorphic garnet is replaced by hornblende, and the marginal portions of magmatic orthopyroxene (pigeonite) crystals are simultaneously replaced by anthophyllite. (b) Blade-shaped biotite flake replacing hornblende in apogabbro amphibolite, zone III. (c) Scapolite veinlet with calcite in the central part (initial scaplotitization). (d) Equilibrium equant scapolite crystals in association with plagioclase, hornblende, and biotite, zone II.

formed into massive *Hbl* ± *Bt* ± *Ath–Pl* ± *Scp* ± *Cal* ± *Qtz* amphibolites.

Zone III: K-Feldspathized Hbl–Bt–Pl–Kfs ± *Scp–Qtz Apogabbroic Amphibolites*

The marginal portion of the metagabbro-norite massif in contact with gneiss-granites (zone III) is altered most significantly. Its principal difference from zone II is the extensive K-feldspathization and silification of the amphibolized basites, which still preserve their melanocratic composition. The potassic feldspar develops first as a metasomatic interstitial mineral (between oligoclase and quartz, Fig. 3b) and veinlets and then gradually expands and forms relatively large grains that belong to the newly formed *Hbl* + *Kfs* + *Pl* ± *Scp* + *Qtz* equilibrium mineral assemblage typical of this zone. The potassic feldspar contents reach 10–15%, and the mineral is poor in the albite end member (1–11%, Table 5). The plagioclase is oligoclase (Table 4). The amount of quartz increases to 10–15%.

Hornblende remains the major mafic mineral of the amphibolites, and its X_{Fe} increases to 0.47–0.55 (Table 6)

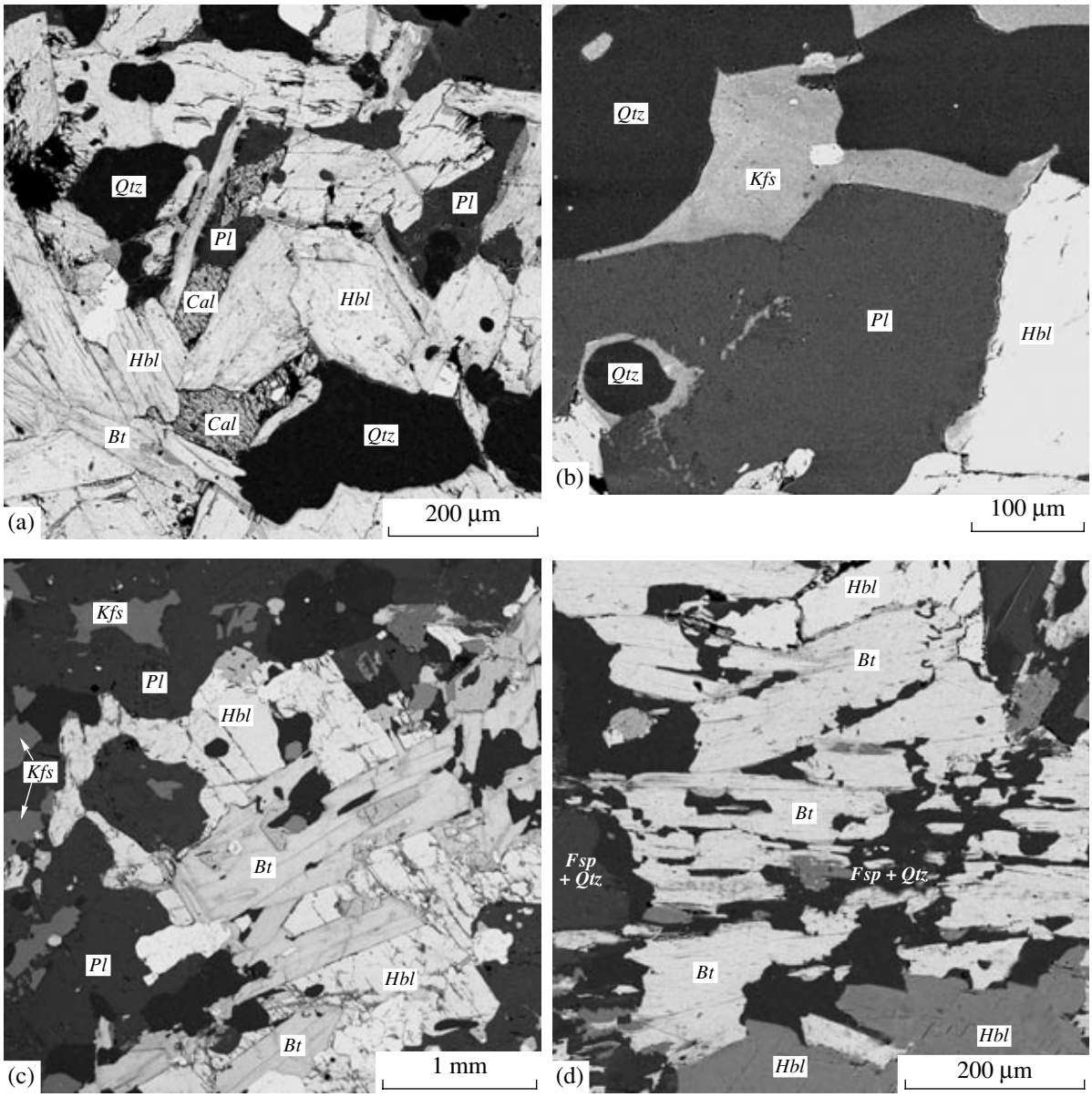

Fig. 3. Amphibolized metagabbro-norites in zones III and IV. (a) Calcite crystals in equilibrium with hornblende, biotite, plagioclase, and quartz in zone III. (b) Interstitial metasomatic potassic feldspar in amphibolite, zone III. (c) Equilibrium relations between hornblende and potassic feldspar and hornblende replaced by biotite in an amphibolite skialith from gneiss-granite. (d) Biotite flake corroded and replaced by a potassic feldspar–plagioclase–quartz aggregate and feldspar and quartz veinlets (microdebasification).

and the composition corresponds to pargasite and ferropargasite. The mineral contains appreciable concentrations of K and is generally rich in both alkalis (Figs. 5, 6). The Cl concentrations in the amphiboles is roughly equal to that in the amphiboles from zone II: up to 0.41 wt %, occasionally up to 0.54 wt %. The amount of biotite, including that replacing hornblende, increases, and its X_{Fe} is as high as 0.43 at an TiO_2 concentration of up to 2.1–3.3 wt % (Table 3). The Cl concentration is up to 0.28 wt %. The amphibolites contain no anthophyllite in association with potassic feldspar.

Scapolitization in zone III is more extensive than in zone II, and the amount of scapolite (which contains 35–51% *Me*, Table 8) reaches 12–15%, although this mineral is unevenly distributed in the rocks, so that some samples contain no scapolite at all. Rounded and amoeba-shaped scapolite grains (which may have replaced oligoclase) are as large as 2–3 mm across and display zoning, with the meionite concentrations increasing from 42 to 51% toward grain rims (Table 8). Occasional calcite grains are in equilibrium with the silicates.

The variations in the chemistries of minerals and their reaction relations suggest the introduction of K, Na, Si, Cl, and CO_2 into the zone-III metagabbroids (they are K-feldspathized, biotitized, oligolcasized, scapolitized, and silicified) and the simultaneous

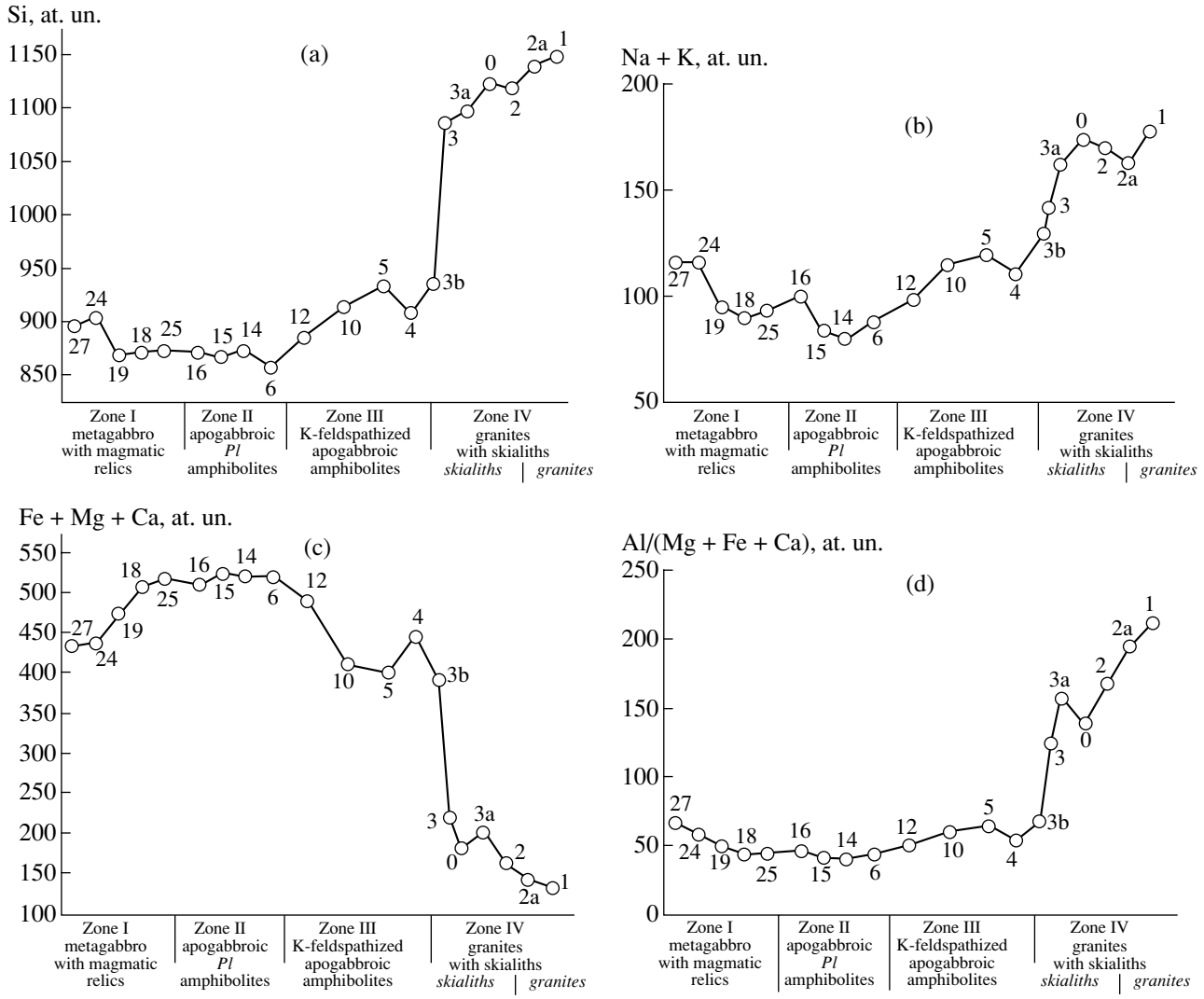

Fig. 4. Variation diagrams for the concentrations of (a) Si, (b) (Na + K), (c) (Fe + Mg + Ca), and (d) the Al/(Mg + Fe + Ca) ratio in the metagabbro-norites with the transition from zone I to zone IV (based on the data of Tables 7 and 8).

removal of Mg (the mafic silicates become more ferrous), Ca (hornblende is partly replaced by biotite), and some Fe. The removal of bases reflects the general tendency toward debasification, i.e., a decrease in the total amounts of mafic minerals at the expense of an increase in the contents of feldspars, scapolite, and quartz, as can also be seen in the variation diagrams (Fig. 4). The summarizing reaction for zone III is

$$Hbl + Olg + SiO_2 + Na_2O + K_2O + H_2O + Cl + CO_2 \longrightarrow Hbl_{>Fe} + Bt_{>Fe} + Kfs + Scp + Qtz \pm Cal + MgO\uparrow + FeO\uparrow + CaO\uparrow. \quad (5)$$

Zone IV: Gneiss-Granites with Skialiths of Bleached Bt–Hbl–Pl–Kfs ± Scp–Qtz Amphibolites

The contact of the marginal part of the metagabbro massif (zone III) with gneiss-granites (zone IV) is sharp, in contrast to the contacts between the first three zones, which grade into one another within the metagabbro-norite body. Within 0.1–1.5 m from the contact, the gneiss-granites that actively interacted with the metabasites contain much skialiths of bleached *Hbl–Bt–Pl–Kfs ± Scp–Qtz* apogabbroic amphibolites (in fact, xenoliths). In spite of the dissolution of the latter in the gneiss-granite migma or magma, they show no traces of thermal transformations (such as the replacement of hornblende with quartz by clinopyroxene–orthopyroxene–plagioclase symplectites or the replacement of biotite with quartz by the orthopyroxene + potassic feldspar assemblage), a fact testifying to the synmetamorphic nature of the gneiss-granites, which were thermally equilibrated with the surrounding amphibolite-facies rocks.

The gneiss-granites have the modal composition *Bt ± Hbl–Pl–Kfs–Qtz*, a gneissose lepidogranoblastic magmatic texture, and equilibrium relations between

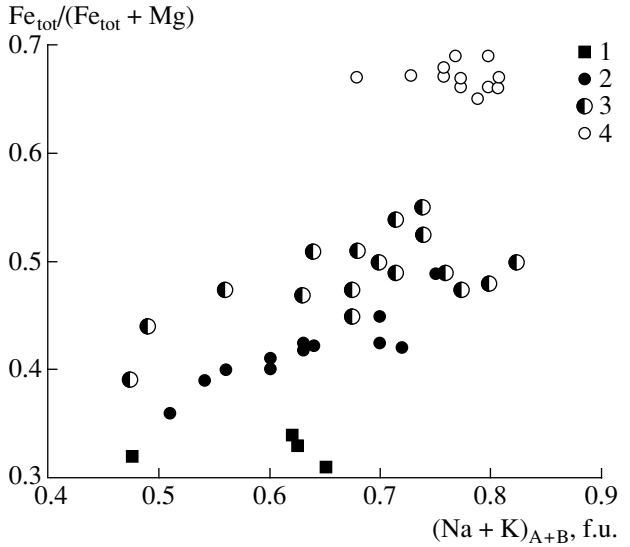

Fig. 5. Variations in the X_{Fe} and the sum of (Na + K) in hornblende with the transition from zone I to zone IV. (1) Weakly amphibolized metagabbro, zone I; (2) apogabbroic plagioamphibolite, zone II; (3) K-feldspathized apogabbroic amphibolite, zone III; (4) gneiss-granite and amphibolite skialiths, zone IV.

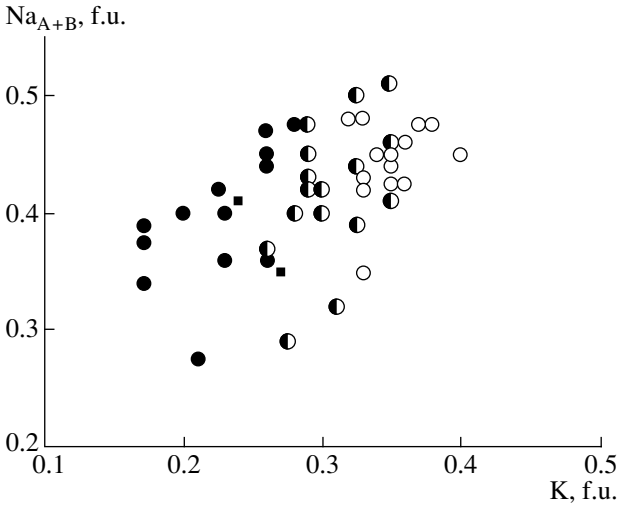

Fig. 6. Variations in the concentrations of Na and K in hornblende with the transition from zone I to zone IV. See Fig. 5 for symbol explanations.

minerals. The total amounts of mafic minerals in these rocks is 4–5%, and these minerals are dominated by ferrous biotite (X_{Fe} = 0.61, sample 1, Table 3) in the form of linearly oriented small flakes. The rarer hornblende forms small prisms of pargasite with X_{Fe} = 0.69. The chemical composition of the gneiss-granite (samples 2a and 1 in Table 10) corresponds to granodiorite according to the classification (Debon and Le Fort, 1983; Baker, 1979). However, the slightly elevated basicity of the granitoid reflects not the granodiorite composition of the melt but the occurrence of small (no larger than 0.5–1.5 cm) amphibolite skialiths in some samples (it was difficult to get rid of these skialiths when samples were prepared for analyses). The gneiss-granites typically show traces of high-temperature autometasomatism: quartz myrmekites at contacts of potassic feldspar and oligoclase, thin albite rims around potassic feldspar, etc.

Megascopically, skialiths of little altered amphibolites are indiscernible from the amphibolites of zone III in the composition of mineral and texture. The further transformations of these rocks in gneiss-granites involves the progressively more extensive hornblende replacement by biotite (Fig. 3c) and the simultaneous resorption of both of these mafic minerals by an oligoclase–potassic feldspar–quartz aggregate or some of its components. As can be seen in Fig. 3d, a biotite flake is corroded and disintegrated by minute "fjords" of *Olg–Kfs–Qtz*, *Kfs–Qtz*, and Qtz composition, a process that ends with the complete dissolution of biotite (and amphibole) in a quartz–feldspar matrix. Thereby the biotite and hornblende show systematic compositional variations. Their X_{Fe} and the K concentration in the amphibole (Figs. 5, 6) further increase, so that the amphibole is transformed into K-rich ferropargasite (X_{Fe} = 0.65–0.69) with slightly lower concentrations of Cl (0.14–0.33 wt %) (Table 6). The X_{Fe} of the biotite also increases, from 0.49 to 0.61 (the Cl concentration is 0.17–0.30 wt %, Table 3). The plagioclase becomes somewhat more sodic (20–22% *An*), and the potassic feldspar contains 4–6% of the albite end member (Tables 4, 5). The amphibolite skialiths contain scapolite, but this mineral is absent from the gneiss-granites.

In the course of their final feldspathization and resorption, the skialiths loose the texture and structure

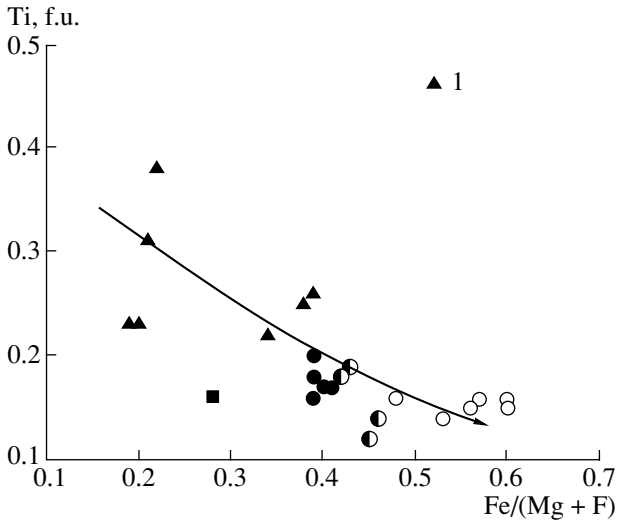

Fig. 7. Variations in the Ti concentration and X_{Fe} of biotite during the recrystallization of magmatic into metamorphic micas in zones I–IV. (1) Magmatic biotite from the gabbronorite. Other symbols are as in Fig. 5.

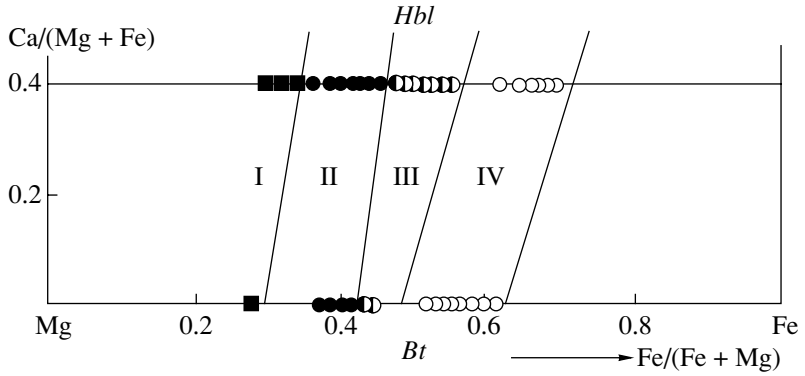

Fig. 8. Variations in the X_{Fe} of coexisting hornblende and biotite with the transition from zone I to zone IV. See Fig. 5 for symbol explanations.

of the amphibolites and are transformed into chains of mesocratic *Bt* ± *Hbl–Kfs–Pl–Qtz* accumulations, which range from 10–15 cm to 1–2 m in length and are parallel to the margin of the gabbro-norite body. The lineation of the large recrystallized biotite flakes is parallel to the gneissosity of the granite.

The summarizing reaction of zone IV is

$$Hbl_{Mg\text{-}Fe} + Bt_{Mg\text{-}Fe} + Olg + K_2O + H_2O + Cl + CO_2 \longrightarrow Bt_{Fe} \pm Hbl_{Fe} + Kfs + Olg_{>Na} + Liq + MgO\uparrow + FeO\uparrow + CaO\uparrow, \quad (6)$$

which describes the complete debasification of the skialiths, in which the X_{Fe} of the amphibole and biotite increases to values typical of these minerals in the gneiss-granites.

Remnants of the skialiths are melted or dissolved in the gneiss-granite, whose basicity does not increase in the inner-contact zone, i.e., no hybridism takes place. This means that the process proceeded in compliance with the classic granitization mechanism, with the complete removal of Mg, Fe, and Ca outside the reaction zone. It is now hard to say which part of the gneiss-granite body with dissolved skialiths corresponded to the semiliquid migma and which was produced by liquid granitic magma. Nevertheless, the process ended with the origin of melt, as also follows from the occurrence of thin pink granite veinlets (up to a few millimeters to 3–4 cm thick and up to 1–5 m long) that branch from the gneiss-granite, penetrate the metagabbro-norite along perpendicular fractures, and gradually taper. These veinlets have thin (5–15 mm) symmetrical amphibolization and biotitization haloes, whose mineral chemistries are identical to those in zones I–III in the metagabbro.

VARIATIONS IN THE BULK-ROCK COMPOSITION OF THE METAGABBRO-NORITES DURING GRANITIZATION (ZONES I–IV)

The bulk-rock compositions of the metagabbro-norites sampled along a profile from the least to the most altered varieties (up to gneiss-granite) (Tables 9, 10) confirm the gradual systematic changes in the composition of these rocks revealed when their mineral assemblage and chemistries were studied.

Analyses of rocks from **zone I** reveal, first of all, the complicating effects of the original microscopic-scale heterogeneity of the gabbroids in the marginal portion of the massif. Since the metasomatic alterations of the metabasites in zone I are of embryonic character, it is reasonable to assume that the differences between the bulk compositions (Fig. 9) are caused in this zone by alternating leucogabbro-norites (analyses 27 and 24) and gabbro-norites (analyses 19, 18, and 25): the latter contain more pigeonite and pigeonite-augite and less plagioclase. This can also bee seen in the variation diagrams (Figs. 4a–4d): the leucogabbro-norites are enriched in silica, alkalis (Na + K), and Ba, have higher X_{Fe} and the Al/(Mg + Fe + Ca) ratios, and are poorer in basic components (Mg + Fe + Ca) and Cr.

Judging from their chemical compositions, the rocks of **zone II** (analyses 16, 15, 14, and 6; Table 9) correspond to recrystallized gabbro-norites but not leucogabbroids, and the overprinted amphibolization almost does not affect their bulk compositions. The (Mg + Fe + Ca) and Si contents and the Al/(Mg + Fe + Ca) ratios of these rocks are practically identical to those of the pristine metagabbro-norites (Fig. 4), as are also their high Cr concentrations (Table 9; compare with the low Cr contents in the leucogabbro-norite of samples 27 and 24, Table 9). However, the overall X_{Fe} of these rocks of zone II, as well as their amphiboles and biotite, increases (Tables 3, 6, 9), which was most probably caused by the higher overall FeO + Fe_2O_3 contents and the somewhat higher X_{Fe} of these magmatic rocks (Table 9). The behavior of alkalis in zone II

is quite unexpected: their concentrations are slightly lower than in the metagabbro-norite (Fig. 4b), most probably because of the lower Al_2O_3 contents in the pristine mafic gabbro-norites of this zone (Table 9). This hindered the crystallization of magmatic and metamorphic plagioclase in these rocks, in spite of the obvious petrographic indications of mild Na introduction into them (amphibolization of pyroxenes). Petrochemical data on these rocks generally do not reveal any traces of the introduction or removal of the major components participating in reaction (4). This suggests only that their migration, a process definitely identified when reaction textures in the zone-II rocks were examined (Figs. 1d, 2a), occurred on a limited scale. At the same time, the fluid-induced reworking the zone-II basites, a process that induced their amphibolization, resulted in a five- to six-fold increase in the Cl concentrations as compared to those in the zone-I rocks (Table 9). This process accounted for the scapolitization of the metagabbro-norites and an increase in Cl contents in their amphiboles and biotite.

The petrochemical trend is drastically modified with the transition to **zone III**. The K-feldspathization, oligoclasizatin, and silicification of the metagabbro-norites result in their enrichment in silica, alkalis, and barium (Table 10). The simultaneous debasification of these rocks is manifested in a decrease in the overall contents of bases (Mg + Fe + Ca), and increase in the Al/(Mg + Fe + Ca) ratio (Fig. 4), and the removal of Cr, an indicator element of gabbroids. The X_{Fe} of the rocks slightly increases, which can be explained, with regard for the general debasification of these rocks, only by the more active removal of Mg than Fe. The Cl concentrations increase, mainly due to scapolitization, because this zone occurs in contact with the gneiss-granite, the source of the Cl-bearing fluid. The petrochemical alterations are not completely even: sample 8 (Fig. 4) deviates from the general tendency and seems to be an "island" of zone-II rocks within zone III.

The metasomatic alterations of the metagabbro-norite are the most intense in **zone IV**, where the alkali enrichment and debasification of the metagabbro skialiths is at a maximum and immediately precedes their complete dissolution in the granitic melt or migma (Fig. 4). The Si, Na + K, and Ba concentrations in them drastically increase, up to the values typical of the gneiss-granite itself (Table 10, sample 1), along with the Al/(Mg + Fe + Ca) ratio and the total iron mole fractions, while the Mg + Fe + Ca contents decrease (Fig. 4), as also do the concentrations of Cr, V, and Ni. These alterations were the final in the process of metagabbroid debasification that was associated with the removal of approximately 80% MgO, 70% CaO, and 60% (FeO + Fe_2O_3) from these rocks (Tables 9, 10). The Cl concentrations in the skialiths and granites decreases because scapolite is unstable in a granitic melt, so that Cl from the fluid can be incorporated only in biotite and/or amphibole, whose contents in the granites are very low.

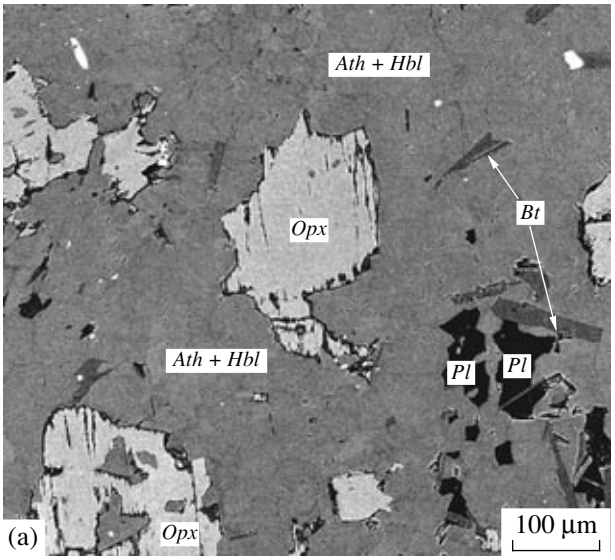

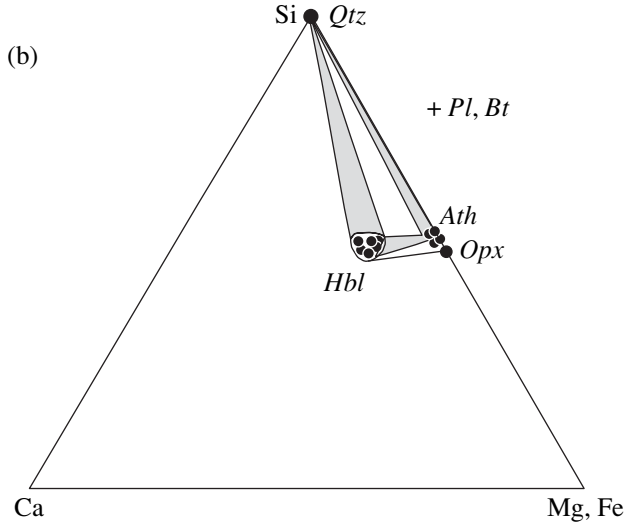

Fig. 9. Equilibrium relations between anthophyllite and orthopyroxene in zone II. (a) *Opx* + *Ath* + *Hbl* + *Bt* + *Pl* mineral assemblage in amphibolite. The orthopyroxene contains no augite lamellae that are typical of the primary pigeonite but contains newly formed hornblende ingrowths. (b) Equilibria between orthopyroxene, anthophyllite, hornblende, and quartz in a Si–Mg, Fe–Ca diagram (mineral chemistries are according to the data of Tables 6 and 7). The *Opx* + *Ath* + *Hbl* mineral assemblage is stable in the absence of *Qtz*, and *Qtz*-bearing rocks contain the *Ath* + *Hbl* + *Qtz* assemblage.

DISTINCTIVE FEATURES OF THE METASOMATIC ALTERATIONS AND THE ENSUING GRANITIZATION OF METAGABBRO-NORITES

The data reported above led us to distinguish the following stages in the contact–metamorphic transformations of metagabbro-norites.

The metabasites composing the relatively large massif were metamorphosed during the Svecofennian cycle, 450–500 m.y. after their emplacement, at T =

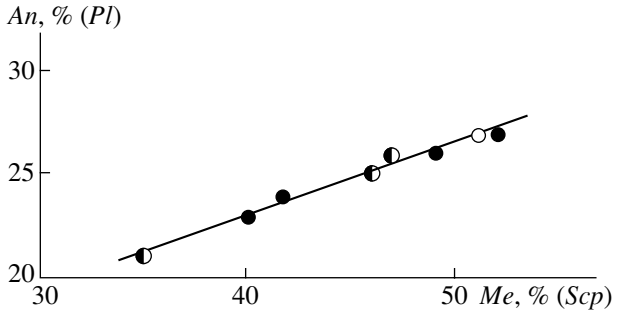

Fig. 10. Correlation between the concentrations of the meionite (*Me*) end member in scapolite (*Scp*) and the anorthite end member (*An*) in plagioclase (*Pl*) in equilibrium pairs of these minerals (Table 8). See Fig. 5 for symbol explanations.

620–670°C and P = 9–10 kbar with formation of quartz-free *Grt–Cpx–Opx–Hbl* assemblages with or without reaction coronas. Our data on these reaction coronas demonstrate that the metamorphism was virtually isochemical (except H_2O). At the culmination of the prograde metamorphism, the metagabbroids in contact with synmetamorphic Svecofennian gneiss-granites were metasomatically transformed under the effect of the metamorphic fluid within a 15-m zone near the contact. During these metasomatic alterations, the bulk chemical and mineralogical compositions of the rocks composing the successive metasomatic zones approached more and more closely the composition of the gneiss-granite. The amphibolized and bleached metabasites were transformed into skialiths in the gneiss-granites, and these skialiths were eventually melted and/or dissolved in the newly formed anatectoid granitic melt.

The metagabbro-norites were reworked under the effect of Cl and CO_2-rich silicic–alkaline solutions, whose high Cl and CO_2 activities follow from the crystallization of scapolite, Cl-bearing amphiboles, and even calcite, all of which are atypical of metasomatic rocks produced during granitization. The elevated Cl activity is a distinctive feature of some Belomorian metasomatic rocks related to Svecofennian migmatites. Some of these rocks contain Cl-bearing pargasite (up to 4.3 wt % Cl) and scapolite (Chukanov et al., 2002).

Since the thickness of the contact–reaction aureole is almost threefold greater than the thickness of the gneiss-granite body itself (4–5 m), it is obvious that the granites were not the source but rather a mediator and the final product of the melting process under the effect of a deep fluid. The latter participated in the migmatization and granitization of the metabasites and their host supracrustal rocks.

Evolution of the Mineral Chemistries

Below we consider, in a generalized form, the mineralogical transformations in the metagabbro-norites that led to a systematic increase in the alkalinity and silicity in the consecutive succession of the zones. The alterations in frontal zone I begin with the nascent replacement of the pigeonite, pigeonite-augite, and corona minerals by **hornblende** rims, a process that ends in zone II with the complete amphibolization and decomposition of the pyroxenes and garnets. Closer to the gneiss-granite, the X_{Fe} of the amphibole increases from 0.31 to 0.69 (Table 6), along with an increase in the contents of alkalis in these minerals and the transformation of the early edenite, magnesiohornblende, and pargasite into ferropargasite. It is worth mentioning that the potassic feldspar-bearing rocks (i.e., those in zones III–IV) contain amphibole with the highest K contents (Fig. 6).

Metamorphic **biotite** starts to crystallize in zone I. First it replaces high-Ti magmatic biotite and develops at the expense of hornblende in zones II through IV (Figs. 2b, 3c). Thereby the X_{Fe} of the biotite systematically increases from 0.28 to 0.61 (Table 3), and its TiO_2 concentrations drastically decrease (Fig. 7) from 6.73 wt % in the magmatic mica to 1.91 wt % in biotite in the gneiss-granite. Consequently, the compositions of the coexisting biotite and amphibole become more ferrous with progress in the metasomatic reworking of the metabasites (Fig. 8).

Low-Al **anthophyllite**, whose X_{Fe} = 25–33% (Table 7) and which first appears in zone I, is spread the most widely in zone II (where it replaces pigeonite), and disappears from the rocks in zones III and IV (see below). Metamorphic **orthopyroxene** equilibrated with anthophyllite and calcic amphibole is also unstable in zones I and II and, in contrast to the magmatic pigeonite replaced by this mineral, bears no augite lamellae (which are recrystallized in hornblende ingrowths).

The evolutionary succession of the **plagioclase** is as follows: labradorite-bytownite is replaced by andesine in zones I and II, and the latter is replaced by oligoclase in zones II–IV, with the most sodic oligoclase formed in skialiths and gneiss-granites (Table 4).

The **scapolite** contains 35–51% of the meionite end member and displays no systematic compositional variations from zone to zone (Table 8, Fig. 10): the composition of this mineral was likely controlled exclusively by the Cl and CO_2 activities in the fluid. Some scapolite crystals are zoned, with the meionite concentration increasing from their cores to margins. Scapolite first appears in zone II, its amount is at a maximum in near-contact zone III, and it disappears from the gneiss-granites (because scapolite is unstable in granitic melts even at high Cl concentrations in the fluid).

Potassic feldspar mildly enriched in Na_2O (Table 4) appears at the boundary between zones II and III, first in the form of secondary interstitial aggregates and then as large individual grains. **Quartz** appears as

minor ingrowths in zone II, and then its amount systematically increases.

Stability of Metamorphic Orthopyroxene and Anthophyllite

During the metamorphism of gabbroids in zones I and II, magmatic pigeonite is replaced not only by hornblende but also by low-Al anthophyllite, and this brings about the *Ath* + *Hbl* + *Bt* + *Pl* and *Opx* + *Ath* + *Hbl* + *Bt* + *Pl* assemblages (Fig. 9a). The *Ath* + *Opx* mineral pair is quite common in CaO-poor metabasites and gneisses of the amphibolite facies within the temperature range of 600–700°C in which these minerals coexist as equilibrium phases (Savolahti, 1966; Korikovsky, 1979; Robinson, 1982). This explains the appearance of any of these minerals in the Belomorian gabbroids similar to norites, in which anthophyllite is produced by the replacement of pigeonite at the introduction of silica and dehydration by the reaction

$$Pig \longrightarrow Ath + Qtz + H_2O. \quad (7)$$

Metamorphic ortopyroxene is produced by the simple partial transformation of pigeonite with the replacement of its augite lamellae by pargasite ingrowths. Considering the compositional similarities between *Ath* and *Opx*, the proportions of these minerals in a rock are controlled exclusively by the amount of silica introduced by the fluid.

This pair is, however, stable only in zones I and II, in quartz- and potassic feldspar-free rocks that were recrystallized at low K and Na activities. The reasons for this are as follows.

(1) *The effect of SiO_2 on the temperature stability of Opx and Ath.* Orthopyroxene is a less silicic phase than anthophyllite, and because of this orthopyroxene appears in silica-undersaturated rocks earlier that in quartz-bearing varieties: at $T \approx 600$°C (Will et al., 1990; Korikovsky and Putis, 2002). Hence, the metamorphic coronas developing in quartz-free Belomorian metagabbro-norites at 640–700°C (Larikova, 2000) contain orthopyroxene but not anthophyllite. Anthophyllite appears later, in place of pigeonite by reaction (7) or instead of coronitic orthopyroxene due to silica introduction into the contact aureole. The effect of SiO_2 on the stability of anthophyllite and orthopyroxene is clearly illustrated in a Si–Ca–Mg, Fe diagram (Fig. 9b): these minerals coexist only in quartz-free metagabbroids, whereas the surrounding quartz-bearing amphibolites contain only anthophyllite but not orthopyroxene.

(2) *The K-feldspathized amphibolites of zones III and IV* contain neither anthophyllite nor orthopyroxene but biotite with quartz, which are formed instead of the former two minerals by the reaction

$$Ath(Opx) + Kfs + H_2O \longrightarrow Bt + Qtz. \quad (8)$$

(3) *At a high Na activity in the fluid*, i.e., in zones III and IV, pigeonite is replaced not by anthophyllite but exclusively by pargasitic hornblende, as is also the case with pigeonite-augite (Fig. 3a)

$$Pig(Opx, Ath) + Lbr\text{-}Anz + Na_2O + H_2O \longrightarrow Hbl_{Prg} + Olg + Qtz. \quad (9)$$

This explains why anthophyllite and orthopyroxene are stable only in the metagabbro-norite of zones I and II (most distant from the gneiss-granite), which still do not contain either quartz or potassic feldspar and in which the activities of alkalis are still relatively low.

Origin of Scapolite at the Granitization Forefront and the Plagioclase–Scapolite Equilibrium

A unique feature of granitization in the Belomorian metagabbroids is the origin of scapolite simultaneously with sodic plagioclase, potassic feldspar, hornblende, biotite, and, sometimes, calcite at the metasomatic forefront. The distribution of scapolite in the rocks of zones I and II is uneven: even metagabbroid samples taken no more than a few centimeters apart can contain from 0 to 15% of this mineral. The likely reason for this was the compositional variations in the Cl- and CO_2-bearing fluid during its percolation through rocks, for example, due to the partial sink of Cl and CO_2 during the crystallization of scapolite, calcite, and Cl-enriched amphiboles and biotite. Thereby each rock domain is characterized by local equilibria between newly formed scapolite (particularly its large euhedral crystals) and nearby plagioclase, as follows from the linear correlation between the concentrations of the meionite and anorthite end members in these minerals (Fig. 10). The origin of zonal scapolite crystals with meionite-richer outer zones suggests that the a_{Cl}/a_{CO_2} ratio in the filtrating fluid gradually decreased during the growth of the scapolite crystals.

This dynamic equilibrium of compositions in the *Pl–Scp* pair depends on the Cl and CO_2 activities (or concentrations) in the filtering fluid. The Na–Ca–Al diagram in Fig. 11 graphically represents the relations between the plagioclase and scapolite solid solutions in equilibrium with a Na-, Cl-, and CO_2-bearing fluid during the scapolitization of metagabbro-norites. The diagram demonstrates why the composition of *Scp* in the *Scp–Pl* pair is more calcic than the composition of the *Pl* and also explains the quantitative proportions of these minerals. For example, when labradorite interacts with a fluid, the following reaction can proceed depending on the activities (or mole fractions) of CO_2 and Cl in the fluid (Fig. 11):

$$Pl\ (50\%\ An) + Na_2O + CO_2 + Cl \longrightarrow Scp\ (50\%\ Me) + Pl\ (40\%\ An)\ (Pl > Scp), \quad (10)$$

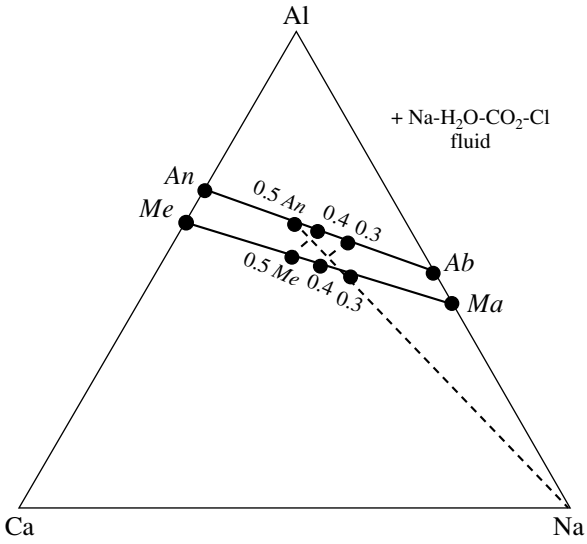

Fig. 11. Evolution of equilibrium between scapolite, plagioclase, and Na–H_2O–Cl–CO_2 fluid during the scapolitization of metagabbro-norites (see text).

$$Pl\ (50\%\ An) + Na_2O + CO_2 + Cl \longrightarrow Scp\ (40\%\ Me) + Pl\ (30\%\ An)\ (Scp > Pl), \quad (11)$$

$$Pl\ (50\%\ An) + Na_2O + CO_2 + Cl \longrightarrow Scp\ (\sim 32\%\ Me)\ (\text{only } Scp, \text{ without } Pl). \quad (12)$$

As the Cl activity increases, these equilibria shift from reaction (10) to reaction (12), i.e., toward greater amounts of scapolite that is progressively richer in its marialite end member.

Scapolite still has never been documented as a mineral crystallizing at the granitization forefront, although synmetamorphic (amphibolite-facies) high-temperature (600–700°C) scapolite-bearing metasomatic rocks with Cl-rich amphiboles produced by the filtration of Cl-bearing high-temperature fluids were described in both the Belomorian series (Chukanov et al., 2002) and elsewhere (Oliver et al., 1994; Markl et al., 1998; Kullerud and Erambert, 1999).

Data on the composition of scapolite in amphibolite skialiths in the zone-IV gneiss-granites were used to constrain the *P–T* metamorphic parameters and identify undeniable evidence of melting in the most debasified, feldspathized, and bleached (up to the level of the gneiss) metagabbroids in this zone. We also attempted to evaluate the composition of the fluid under the assumption that its composition can be realistically enough approximated by an H_2O–CO_2–NaCl mixture (Khodorevskaya, 2005). Melting in the granite–CO_2–H_2O system at $T \approx 640$–700°C and $P \approx 10$–11 kbar corresponds to $a_{H_2O} \approx X_{H_2O} \approx 0.6$ (Ebadi and Johannes, 1991). The NaCl mole fraction in the fluid can be quantified with regard for the average composition of the scapolite (≈40% *Me*) in amphibolite skialiths from the gneiss-granites. The calculations with the use of experimental data on the reaction $NaCl_{Scp} + CaCO_{3\,Cal} = CaCO_{3\,Scp} + NaCl_{Fl}$ (Ellis, 1978) yielded $X^{Fl}_{NaCl} \approx 0.25$–0.35 for fluid in equilibrium with the scapolite-bearing amphibolites in skialiths. This means that **the fluid in zone IV was a highly concentrated chloride brine.**

General Evolutionary Succession of the Granitization Process in the Belomorian Metagabbro-Norites

The succession of mineral replacements during the closing stages of the reworking of the skialiths in the gneiss-granite melt was described above. The principal geochemical tendency of this final process, which is granitization itself, is the bleaching of once melanocratic amphibolite skialiths, their transformation, first, into mesocratic and then leucocratic *Bt–Hbl–Fsp–Qtz* nebular rocks and, eventually, complete dissolution in the granitic melt under the effect of the continuing fluid flow percolating through the granitic magma. As a result, the amount of the melt increases, while the amount of the metagabbro in the reaction zone simultaneously decreases. The general changes in the mineral assemblages in the contact aureole are displayed in Fig. 12, which clearly demonstrates the infiltration character of the process with an increase in the Al/(Mg + Fe + Ca) ratio of the rocks. Thereby Mg, Fe, and Ca, which are excess components with respect to the granitic eutectic, are completely removed, so that more basic inner-contact facies is not formed in the gneiss-granites. No basificates, melanocratic *Hbl–Bt* rims, or the products of Fe–Mg–Ca vein or frontal metasomatism were found in the peripheral part of the reaction zone, in contact with the metabasite massif, or within it. Hence, the excess basic components migrated far away from the reaction site, and the granitization process occurred there in its pure form, in full compliance with Korzhinskii's (1976) model. Analogous processes and phenomena were documented elsewhere within the fields of Belomorian rocks (Shcherbakova, 1988; Beus et al., 1993).

This does not mean at all that related basificates can never be produced in principle: here we mean only the geological contact described in this paper. For example, in the Belomorian metamorphic complex in Kii Island, porphyroblastic nebular migmatites in the peripheral portions of granitic bodies are cut by subconformable veins of coarse-grained *Grt–Hbl–Bt* ± *Cpx* ± *Pl* rocks, whose genesis cannot be explained otherwise but by vein Fe–Mg–Ca metasomatites. The source of the material remains uncertain and presumably occurred at a certain depth, but it was most probably complementary with the granitization of the metabasites. Analogous basic metasomatic rocks related to granitization were described in the Belomorian Complex (Terekhov et al., 1997) and elsewhere (Petrova and Levitskii, 1984; *Iron–Magnesian Metasomatism…*, 1980).

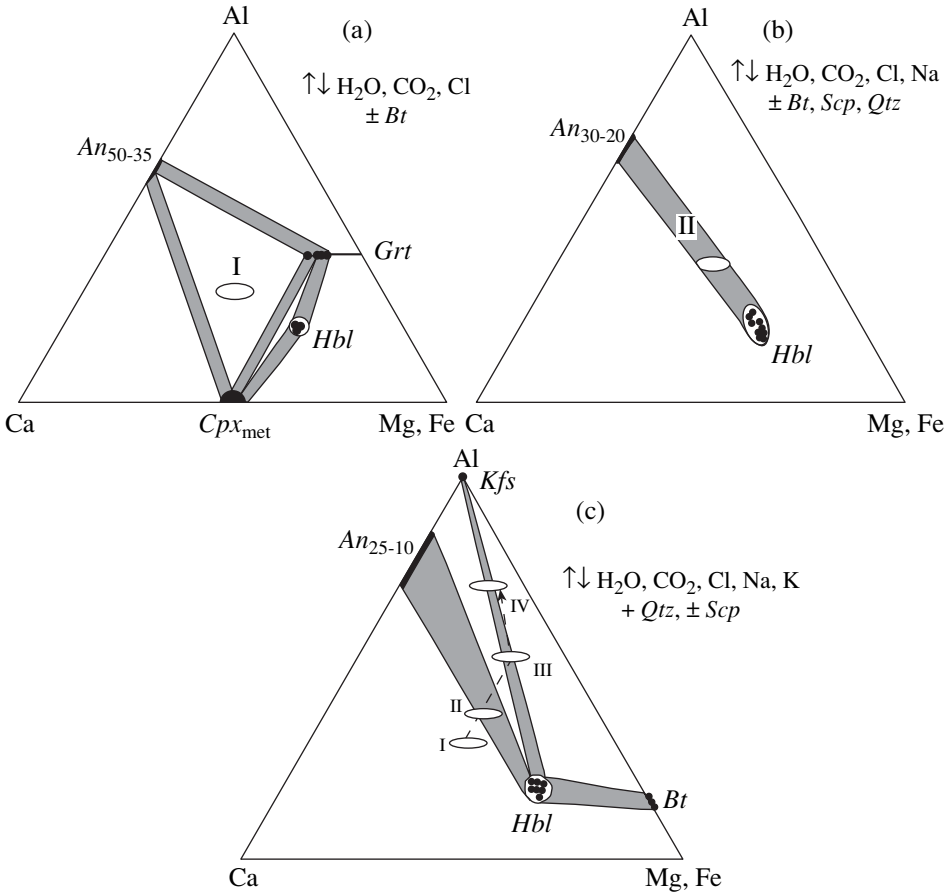

Fig. 12. ACF diagram showing the evolutionary succession of mineral assemblages in metagabbro-norites during their granitization. (a) Zone I (inert alkalis); (b) zone II (Na is perfectly mobile); (c) zones III and IV (both Na and K are perfectly mobile).

The granitization of the metagabbro-norite considered above is closely similar to the transformations of small and large metabasite bodies in various migmatized metamorphic complexes (Engel and Engel, 1958; Volokhov and Ivanov, 1968; Krylova et al., 1972; Petrova and Levitskii, 1984; Zharikov and Gavrikova, 1987; Gavrikova and Zharikov, 1984; Gavrikova, 1987; Shcherbakova, 1988). The process is usually subdivided into two stages.

During the first stage, under amphibolite-facies parameters, the percolation of silicic–alkaline fluids across the contact with the granites caused the progressively more extensive metasomatic reworking of the metabasites (para- and orthoamphibolites, metagabbro, two-pyroxene crystalline schists, and others), a process associated with the replacement of the primary mafic minerals by progressively more ferrous Na- and K-bearing phases (biotite and hornblende) and the replacement of calcic plagioclase by more alkaline Na–Ca and K-feldspars and quartz. This debasification caused the gradual leaching of significant Mg, Fe, and Ca amounts from these rocks, which became transformed into more leucocratic rocks enriched in Na, K, and Si and containing newly formed interstitial sodic plagioclase, potassic feldspar, and quartz. The metasomatic feldspathization that preceded the melting of the rocks occurred independently of the metamorphic temperature, in both the granulite and amphibolite facies. However, under granulite-facies conditions, potassic-feldspar and quartz–potassic feldspar metasomatism does not decompose granulite-facies minerals and produces the *Opx + Kfs* charnockite mineral assemblages (Korikovsky, 1967; Franz and Harlov, 1998; Harlov et al., 1998; Harlov and Wirth, 2000) without significant biotitization or amphibolization. If the process is more active, granulite-facies feldspathization and silification also result in the debasification of the metamorphic rocks before the development of nebular *Opx–Kfs* migmatites and the ensuing melting of *Opx–Kfs* charnockites (Perchuk et al., 1994, 2000).

During the second stage of granitization, the alkalinized metabasites are disintegrated into fragments in the form of skialiths, which are transformed into progressively more meso- and leucocratic nebular aggregates in the course of this process. With the onset of their partial melting, they give rise, first, to semiliquid migma and, then, to a granitic melt or simply dissolve in the nearby gneiss-granite. This evolutionary process

resulted in the gradual replacement of amphibolite layers and/or metabasite bodies by nebular *Bt–Hbl* migmatites or gneiss-granites under amphibolite-facies conditions (Korikovsky, 1967; Zharikov and Gavrikova, 1987; Gavrikova and Zharikov, 1984; Gavrikova, 1987; Beus et al., 1993; Matveeva, 1976; Shcherbakova, 1988).

The general succession of the mineral equilibria during the granitization of metagabbro-norites of the Belomorian Complex is shown in Fig. 12. Frontal zone I contains preserved regional-metamorphic assemblages under the nearly inert behavior of alkalis. The rear part of zone II is marked by mild debasification, with Na inflowing into this zone behaving as a perfectly mobile component. The fluid in this zone was depleted in K, because this element was precipitated in zone III. The fluid in zones III and IV was a Na–K–H_2O–CO_2–Cl brine. These zones are characterized by the maximum debasification, and because of the leaching and a decrease in the bulk-rock concentrations of bases at an inert behavior of Al, the Al/(Ca + Mg + Fe) ratio of the rocks increases. Alkalis behave as perfectly mobile components in zones III and IV at the most significant action of the fluid and during initial melting (in zone IV).

THE ROLE OF GRANITIZATION AS A MAGMA-GENERATING PROCESS AND THE GENESIS OF FLUIDS

The model of granitization provides insight into many phenomena that cannot be explained within the framework of the model for anatexis in a closed system. Only the existence of independent, not related to the contacts of any granitic massifs, fluid flows makes it possible to explain the vast scale of the silicic–alkaline metasomatism (feldspathization, biotitization, silification, and pegmatitization) that occurs over huge areas within permeable zones at all ancient crystalline shields (Sudovikov, 1964). Silicic–alkaline fluids actively affected all rocks, particularly those of basic composition, and induced their debasification and melting. The leached basic components were mostly not precipitated at the anatexis forefront in the form of Fe–Mg–Ca metasomatites but were removed outside the zones of granite formation and migmatization, a feature that illustrates the infiltration-controlled (but not diffusion-controlled) character of the process. Silicic–alkaline metasomatism can produce only quartz–feldspar metasomatites and feldspathized rocks without any traces of their melting. However, if the circulation of the fluids (more specifically, Na-, K-, and Si-rich H_2O–Cl–CO_2 brines; Aranovich and Newton, 1998; Newton et al., 1998) was more intense and lasted for a longer time, the metabasites were transformed first into nebular migmatites, then into a migma, and were finally replaced by a tonalite or two-feldspar granitic melt (depending on the composition of the fluid). The latter was clearly demonstrated by Shcherbakova (1988) with reference to the example of the granitization of amphibolites in the Belomorian series. After this final stage of the process, the newly formed anatectic products merged into larger homogeneous bodies, which formed variably sized granite-gneiss domes. The volumes of the latter at shields always increases, while the volumes of metabasite rocks simultaneously decrease. Because of this, the general geochemical vector in the evolution of all ancient shields is always their debasification and granitization.

Anatexis in a closed system should lead to fundamentally different results. First of all, this process cannot in principle produce nebular migmatites or any products of debasification, bleaching, or alkaline metasomatism, particularly in metabasite rocks. The simple differentiation of a rock into leucosomes and melanosomes should have resulted in banded complexes (if the acid melts were not removed) or, if the silicic–alkaline melts migrated into higher levels, in the progressively stronger "autobasification" (but not granitization) of ancient shield, which is in conflict with the actual geochemical evolution of these shields.

Anatexis in a closed system (for example, in metabasites) should produce droplets of partial granitic melts. These droplets should have a granophyric texture and be submerged into a melanocratic rock mass. The latter should also contain traces of pathways used by the melts for their ascent, so that the leucosome should inevitably display passive relations with the melanosome. However, naturally occurring migmatites, particularly those of the amphibolite facies, more commonly exhibit opposite relations: the melanosomes are actively affected by the leucosomes, thin rims of biotitization and feldspathization (alkalinization) develop at the contacts of metabasites, and the melanosomes are corroded by acid melts or silicic–alkaline fluids with an unambiguous tendency of the transformation of the melanosome into feldspathized skialiths. Along with the lateral heterogeneity of the degrees of melting of compositionally diverse rocks, this demonstrates the participation of an external fluid in the process.

Experimental data on the melting of amphibolites in a closed system (Rapp, 1995; Rushmer, 1991; Khodorevskaya and Zharikov, 1998) indicate that, if all water is supplied to the melt by the decomposition of amphiboles and biotite, the solidus temperature of plagiogranites is no lower than 800°C. In this situation, the partial melting of amphibolites can occur only under granulite-facies conditions. A temperature decease to 650–700°C, i.e., to the parameters of the amphibolite facies, can take place only at higher contents of aqueous fluids (Vielzeuf and Schmidt, 2001), which can come into naturally occurring metabasites only from the outside, thus reflecting the openness of the system (Khodorevskaya, 2006).

Thus, the study of natural metamorphic complexes, including those with metabasites, and experimental data on their melting indicates that the anatectic forma-

tion of granites occurred in them usually in open systems, which corresponded to the granitization model (Korzhinskii, 1952, 1976; Beus et al., 1993; Volokhov and Ivanov, 1968; Gavrikova, 1987; Zharikov, 1987, 1996; Zharikov and Gavrikova, 1987; Zhdanov, 1959; Korikovsky, 1967; Krylova et al., 1972; Kuznetsov and Izokh, 1969; Lashkevich, 2002; Letnikov et al., 1988, 2000; Letnikov, 2002; Marakushev, 2002; Matveeva, 1976; Milovskii et al., 1985; Perchuk et al., 2000; Khodorevskaya, 2006; Shcherbakova, 1988; Engel and Engel, 1958; Olsen, 1982, 1984, 1985).

Petrological Evidence of Mantle Fluid Inflow during Metamorphism and Granitization

A mantle source of fluids during metamorphism and granitization is evident from the occurrence of regional diaphthoresis of the Archean granulites composing ancient shields. For example, the Paleoproterozoic diaphthoresis of lower crustal "dry" Archean granulites and charnockites in the Aldan Shield, Anabar Massif, and the Stanovaya zone under amphibolite-, epidote-amphibolite-, and greenschist-facies conditions affected vast areas of hundreds and thousands of square kilometers and was associated with granitization with the derivation of biotite–muscovite granites (Korzhinskii, 1939; Sudovikov et al., 1965; Korikovsky, 1967; Lutts, 1964). This process required the inflow of vast volumes of fluids from beneath the "granulite" depth level. According to the model of plate tectonics, water is supplied to the mantle by the subduction of large volumes of water-bearing sedimentary rocks. Their dehydration should bring about "secondary" mantle fluids, which participate in the derivation of water-bearing mantle magmas and, when ascending, cause the diaphthoresis of high-temperature crustal rocks. This explanation is absolutely inapplicable to the diaphthoresis at Archean granulite shields (such as the Aldan Shield or the Anabar Massif), because there is no geological or geophysical evidence of the subduction of any Proterozoic sedimentary sequences (as a potential source of fluids) beneath ancient granulite shields. Moreover, the results obtained by Ferry (1994) indicate that the metamorphism of even water-bearing sedimentary rocks requires that each unit volume of the rock was penetrated by two- to threefold greater volumes of fluid. The diaphthoresis of dry granulites and charnockites requires an even higher volumes of percolating fluids. This can be explained only under the assumption that the fluids can be provided exclusively by mantle sources. It was the studying of diaphthoresis in the Archean granulites of the Stanovaya zone that led D.S. Korzhinskii (1952) to his hypothesis of deep transmagmatic solutions.

Evidence that CO_2- and H_2O-Bearing Fluids Can Be Generated in the Mantle

Carbon dioxide. Data obtained on mantle xenoliths in basalts indicate that mantle material often contains carbonates in equilibrium with mantle phases. These carbonates can be present in the form of both equant grains and veinlets (Ionov et al., 1993; Kogarko et al., 2001), with the latter regarded as traces of mantle metasomatism under the effect of CO_2-bearing fluids. The CO_2 concentration in mantle domains from which protokimberlite melts are derived can be as high as 15–20% (Ryabchikov, 2005), which provides the basis for models for the generation of mantle carbonatite and kimberlite magmas (Ryabchikov, 2005; Kogarko, 2005). Independent CO_2 emanations coming into the Earth's crust early in the Earth's history, from the Archean to Paleoproterozoic, could be produced by the oxidation of mantle carbon (Galimov, 2005). The resultant flows of fluid strongly enriched in CO_2 penetrated the overlying crust and could play, according to Galimov, a decisive role in the generation of Archean granulites over extensive areas at ancient shields, because the fluids of granulite metamorphism are often thought (Newton, 1986) to have been characterized by much higher activities (or concentrations) of CO_2 than H_2O. All of these considerations and facts demonstrate that the mantle could serve as a powerful source of CO_2-bearing fluids, a feature that strongly affected metamorphism and granitization in the Early Precambrian.

Water. The processes of metamorphism or eclogitization of the lower crust in the basements of ancient shields could not proceed without intense inflow of aqueous fluids from the mantle (it is difficult to imagine other sources of these fluid at that time). This finds support in geodynamic evidence: according to Artyushkov (2002, 2003), the only realistic reason for the softening of originally rigid lithospheric plates that enabled their plastic extension or compression were fluid emanations from the underlying asthenosphere. These deep CO_2–H_2O fluids, which were initially in equilibrium with the peridotite mantle (Schneider and Eggler, 1986), are characterized by extremely high solubility of SiO_2, K_2O, and Na_2O (Zharikov, 2002). Their saturation with leucocratic components occurred when these fluids interacted with lower crustal silicic rocks. Percolating to higher levels, these fluids were modified into silicic–alkaline H_2O–CO_2 brines (Aranovich and Newton, 1998; Newton et al., 1998) and could cause the intense metasomatic reworking and granitization of metamorphic rocks, for example, metabasites.

Calculations indicate that the modern silicate mantle contains fairly low overall amounts of volatile components (which are mostly oxidized) (Ryabchikov, 2003): 0.1 wt % H_2O, 0.08 wt % CO_2, and 0.002 wt % Cl. These concentrations are even lower in the depleted and degassed mantle. According to I.D. Ryabchikov, the overall concentrations of volatiles (including water that

was incorporated into anhydrous silicates of the olivine type) in the mantle cannot exceed 0.3–0.4%, which imposes constraints on the possibility of the generation of significant amounts of mantle fluids. This conclusion pertains to the Phanerozoic and modern depleted mantle. However, practically all researchers admit that the early evolution of the Earth, up to the Archean–Paleoproterozoic boundary, was characterized by the existence of reduced volatiles that were rich in hydrogen. This model was explored in detail by Letnikov (1998, 2002). According to it, hydrogen that separated from the mantle during its primary degassing in the Early Precambrian interacted with the oxygen-rich shell and gave rise to water, simultaneously with the appearance of carbon dioxide from oxidizing mantle carbon (Galimov, 2005). This process could generate H_2O–CO_2 fluids. The transition from reduced to oxidizing conditions in the Early Precambrian was responsible for the origin of large volumes of H_2O–CO_2 fluids. These fluids actively filtrated through rocks and induced their high-temperature metamorphism and granitization over vast areas in Archean and Paleoproterozoic complexes.

CONCLUSIONS

1. The results of our research demonstrate that the granitization of the metagabbro-norites occurred at the culmination of the Svecofennian high-pressure metamorphism of the gabbroids and their host rocks of the Belomorian Complex at T = 660–700°C and P = 9.5–10.5 kbar.

2. The alterations affected the marginal part of the metagabbro massif, in contact with synmetamorphic *Bt* ± *Hbl–Kfs–Pl–Qtz* gneiss-granites within a 15- to 20-m zone, under the effect of a flow of silicic–alkaline H_2O–Cl–CO_2 brines, which were associated with and genetically related to the gneiss-granites.

3. The action of the fluids in the reaction zone was of unidirectional character and reflected the infiltration-controlled type of the process. The metagabbroids were thereby gradually enriched in Na, K, Si, Cl, CO_2, and H_2O and depleted in Ca, Mg, Fe, and Cr, which were redeposited outside the reaction zone (there are no Fe–Mg–Ca metasomatic rocks near it). These alterations are illustrated in variation diagrams based on chemical analyses of the rocks.

4. The intensity of alterations in the metagabbroids gradually increased toward the contact with gneiss-granites, as is pronounced in the replacement of magmatic and corona minerals by hornblende, biotite, anthophyllite, oligoclase, potassic feldspar, scapolite, and quartz. According to the systematic changes in the mineral assemblage and the bulk compositions of the rocks, the contact–reaction interval can be subdivided into the following four zones: (I) weakly amphibolized metagabbro-norites; (II) apogabbroic *Hbl–Pl* ± *Scp* ± *Qtz* plagioamphibolites with *Hbl*, *Bt*, *Ath*, *Olg*, and *Scp* rims around magmatic and coronitic minerals; (III) K-feldspathized *Hbl–Bt–Pl–Kfs* ± *Scp–Qtz* apogabbroic amphibolites; and (IV) *Bt* ± *Hbl–Kfs–Pl–Qtz* gneiss-granites with skialiths of bleached *Bt–Hbl–Pl–Kfs* ± *Scp–Qtz* amphibolites. These transformations reflect the progressive alkali enrichment and debasification of the metagabbro-norites.

5. With the intensification of the process, the compositions of the newly formed minerals systematically varied. The hornblende became more ferrous (its X_{Fe} increased from 0.31 to 0.69) and more alkaline; its K/Na ratio increased. The biotite also became much more ferrous (X_{Fe} increases from 0.28 to 0.61) and less titanian compared to the primary magmatic biotite. The concentration of the anorthite end member in the plagioclase decreased from 60–80 to 20–22%. The chemistry of the scapolite depended not on the zone but on the CO_2 and Cl concentrations in the fluid, and the concentration of the meionite end member varied in this mineral from 30 to 50%. Scapolite crystallized at the peak of the process and displays equilibrium relations with the plagioclase.

6. The alterations in zones I–III are of purely metasomatic character. In zone IV, fragments of bleached metagabbro-norites are separated from the main body and are transformed into skialiths in the gneiss-granites. The further debasificatin of these skialiths is associated with a gradual decrease in their sizes due to dissolution and melting in the granitic migma or magma. It is hard to megascopically distinguish between the newly formed migma and magma with numerous small (from 2 to 40–50 mm) skialiths of the apogabbroic amphibolites. The origin of a melt is obviously evident from the occurrence of thin (0.5–2 cm) granitic veinlets, which branch from the gneiss-granite and cut across the marginal part of the metagabbroid massif, running perpendicular to its contact with the gneiss-granite.

7. We managed to distinguish all stages of the granitization of metagabbroids in this aureole. The relations and tendencies identified in it are in good agreement with the well-known model proposed by D.S. Korzhinskii.

ACKNOWLEDGMENTS

The authors thank E.V. Sharkov (Institute of the Geology of Ore Deposits, Petrography, Mineralogy, and Geochemistry, Russian Academy of Sciences) for the constructive discussion of the results obtained during this research and valuable help with the fieldwork. This study was financially supported by the Russian Foundation for Basic Research, project nos. 05-05-64831 and 06-05-64645.

REFERENCES

1. N. L. Alekseev, S. B. Lobach-Zhuchenko, and E. S. Bogomolov, “Phase and Nd Isotopic Equilibria in Drusites of Cape Tolstik and the Tupaya Bay Area, Northwestern

Belomorie, Baltic Shield," Petrologiya **7**, 3–23 (1999) [Petrology **7**, 1–20 (1999)].

2. L. Y. Aranovich and R. C. Newton, "Reversed Determination of the Reaction: Phlogopite + Quartz = Enstatite + Potassium Feldspar + H_2O in the Ranges 750–875°C and 2–12 kbar at Low H_2O Activity with Concentrated KCl Solutions," Am. Mineral. **83**, 193–204 (1998).
3. E. V. Artyushkov, "Large-Scale Tectonic Movements in Ultra-High Pressure Metamorphism on Continents as a Consequence of the Infiltration of Surface-Active Fluids from Mantle Plumes into the Lithosphere," in *Proceedings of All-Russian Symposium on Fluid Flows in the Earth's Crust and Mantle, Moscow, Russia, 2002* (Moscow, 2002), pp. 51–55 [in Russian].
4. E. V. Artyushkov, "Abrupt Continental Lithosphere Weakening as a Precondition for Fast and Large-Scale Tectonic Movements," Geotektonika, No. 2, 39–56 (2003) [Geotectonics **37**, 107–123 (2003)].
5. F. Barker, "Trondhjemite: Definition, Environment and Hypothesis of Origin," in *Trondhjemites, Dacites and Related Rocks*, Ed. by F. Barker (Elsevier, Amsterdam, 1979), pp. 1–12.
6. A. A. Beus, T. F. Shcherbakova, and L. N. Kuklei, "Geochemical Features of Granitization and the Average Composition of Rocks of the Belomorian Complex," in *Geochemical Evolution of Granitoids in the Lithospheric Evolution* (Nauka, Moscow, 1993), pp. 69–94 [in Russian].
7. E. V. Bibikova, S. V. Bogdanova, V. A. Glebovitsky, et al., "Evolution of the Belomorian Belt: NORDSIM U–Pb Zircon Dating of the Chupa Paragneisses, Magmatism, and Metamorphic Stages," Petrologiya **12**, 227–244 (2004) [Petrology **12**, 195–210 (2004)].
8. N. V. Chukanov, A. N. Konilov, A. E. Zadov, et al., "New Amphibole Potassic Chlorine-Pargasite $(K,Na)Ca_2(Mg,Fe^{2+})_4Al(Si_6Al_2O_{22})(Cl,OH)_2$ and the Formation Conditions in the Granulite Complex of Sal'nye Tundras, Kola Peninsula," Zap. Vseross. Mineral. O–va, No. 2, 58–62 (2002).
9. F. Debon and P. Le Fort, "A Chemical–Mineralogical Classification of Common Plutonic Rocks and Associations," Trans. R. Soc. Edinburgh Earth Sci. **73**, 135–149 (1983).
10. A. Ebadi and W. Johannes, "Beginning of Melting and Composition of First Melts in the System *Qtz–Ab–Or–*H_2O–CO_2," Contrib. Mineral. Petrol. **106**, 286–295 (1991).
11. J. O. Eckert, R. C. Newton, and O. J. Kleppa, "The ΔH of Reaction and Recalibration of Garnet–Pyroxene–Plagioclase–Quartz Geobarometers in the CMAS System by Solution Calorimetry," Am. Mineral. **76**, 148–160 (1991).
12. D. M. Ellis, "Stability and Phase Equilibria of Chloride- and Carbonate-Bearing Scapolites at 750°C and 4000 bar," Geochim. Cosmochim. Acta. **42**, 1271–1281 (1978).
13. A. E. J. Engel and C. G. Engel, "Progressive Metamorphism and Granitization of the Major Paragneiss, Northwest Adirondack Mountains, New York. Part 1. Total rocks," Bull. Geol. Soc. Amer. **69**, 1369 (1958).
14. J. M. Ferry, "A Historical Review of Metamorphic Fluid Flow", J. Geophys. Res. **99**, 15487–15498 (1994).
15. L. Franz and D. E. Harlov, "High-Grade K-feldspar Veining in Granulites from the Lower Crust and Implications for the Granulite Facies Genesis," J. Geol. **106**, 455–472 (1998).
16. E. M. Galimov, "Redox Evolution of the Earth Caused by a Multi-Stage Formation of its Core," Earth Planet. Sci. Lett. **233**, 263–276 (2005).
17. S. N. Gavrikova and V. A. Zharikov, "Geochemical Features of the Granitization of Archean Rocks in Eastern Transbaikalia," Geokhimiya, No. 1, 26–49 (1984).
18. S. N. Gavrikova, "Early Proterozoic Granitization in the Southern Part of the Aldan–Vitim Shield," in *Contributions to Physicochemical Petrology* (Moscow, 1987), pp. 64–90.
19. D. E. Harlov and R. Wirth, "K-Feldspar–Quartz and K-Feldspar Phase Boundary Interactions in Garnet–Orthopyroxene Gneisses from the Val Strona di Omegna, Ivrea–Verbano Zone, Northern Italy," Contrib. Miner. Petrol. **140**, 148–162 (2000).
20. D. E. Harlov, E. C. Hansen, and C. Rigler, "Petrologic Evidence for K-Feldspar Metasomatism in Granulite Facies Rocks," Chem. Geol. **151**, 373–386 (1998).
21. D. A. Ionov, C. Dupuy, S.Y. O'Reilly, et al., "Carbonated Peridotite Xenoliths from Spitsbergen: Implications for Trace Element Signature of Mantle Carbonate Metasomatism," Earth Planet. Sci. Lett. **119**, 283–297 (1993).
22. *Iron–Magnesian Metasomatism and Ore Formation*, Ed. by V. A. Rudnik (Nauka, Moscow, 1980) [in Russian].
23. L. I. Khodorevskaya and S. P. Korikovsky, "Contact–Reaction Interaction between Gneiss Granites and Coronitic Gabbro in the Belomorian Complex as an Example of Granitization of Metamafic Rocks: Evidence from Kandalaksha Bay, Gorelyi Island," in *Proceedings of International (10th All-Russian) Petrographic Conference "Petrography in the 21th Century", Apatity, Russia, 2005* (Apatity, 2005), Vol. 3, pp. 265–267 [in Russian].
24. L. I. Khodorevskaya and V. A. Zharikov, "Experimental Study of Amphibolite Melting and Relation with Problems of Genesis of Tonalite–Trondhjemite Series," in *Experimental and Theoretical Modeling of Mineral Formation* (Nauka, Moscow, 1998), pp. 11–31 [in Russian].
25. L. I. Khodorevskaya, Doctoral Dissertation in Geology and Mineralogy (Mosk. Gos. Univ., Moscow, 2006).
26. L. I. Khodorevskaya, "Fluid Regime during the Granitization of Coronitic Metagabbros in the Belomorian Complex: Reconstruction Based on Scapolite-Bearing Assemblages," in *Proceedings of Conference on Belomorian Mobile Belt and It's Analogues: Geology, Geochronology, Geodynamics, and Metallogeny, Petrozavodsk, Russia, 2005* (Petrozavodsk, 2005), pp. 314–316 [in Russian].
27. L. N. Kogarko, "Role of Global Mantle Metasomatism and Genesis of Alkaline, Carbonatite, and Kimberlite Magmatism," in *Proceedings of International Symposium on Evolution of the Continental Lithosphere, Origin of Diamonds and Their Deposits, Novosibirsk, Russia, 2005* (Sib. Otd. Ross. Akad. Nauk, Novosibirsk, 2005), p. 90 [in Russian].
28. L. N. Kogarko, G. Kurat, and T. Ntaflos, "Carbonate Metasomatism of the Oceanic Mantle beneath Fernando

de Noronha Island, Brazil," Contrib. Miner. Petrol. **140**, 577–587 (2001).

29. M. Y. Kohn and F. S. Spear, "Two New Geobarometers for Garnet Amphibolites, with Application to Southeastern Vermont," Am. Mineral. **75**, 89–96 (1990).
30. S. P. Korikovsky and M. Putič, "Olivine–Orthopyroxene–Amphibole–Talc–Chlorite Metaserpentinites in the Medium-Temperature Metamorphic Complex of Northern Veporic, Western Carpathians: Phase Relations, Metamorphic Parameters, Comparison with Gneiss and Amphibolite Associations," Petrologiya **10**, 3–29 (2002) [Petrology **10**, 1–22 (2002)].
31. S. P. Korikovsky, *Metamorphic Facies of Metapelites* (Nauka, Moscow, 1979) [in Russian].
32. S. P. Korikovsky, *Metamorphism, Granitization, and Post-Magmatic Processes in the Precambrian of the Udokan–Stanovoi Zone* (Nauka, Moscow, 1967) [in Russian].
33. S. P. Korikovsky, "Reaction Phase Equilibria during the Recrystallization of Paleoproterozoic Gabbronorites of the Belomorian Complex under Conditions Close to the Amphibolite–Eclogite Facies Boundaries," in *Proceedings of Scientific Conference on the Belomorian Mobile Belt and It's Analogues: Geology, Geochronology, Geodynamics, and Metallogeny, Petrozavodsk, Russia, 2005* (Petrozavodsk, 2005), p. 189–191.
34. D. S. Korzhinskii, "Precambrian of the Aldan Plate and Stanovoi Range" in *Stratigraphy of USSR* (Akad. Nauk SSSR, Moscow, 1939), Vol. 2, pp. 349–366 [in Russian].
35. D. S. Korzhinskii, "Granitization as Magmatic Replacement," Izv. Akad. Nauk SSSR, Ser. Geol., No. 2, 332–452 (1952).
36. D. S. Korzhinskii, "Transmagmatic Fluids and Magmatic Replacement," in *Petrography* (Mosk. Gos. Univ., Moscow, 1976), Part 1, pp. 117–129 [in Russian].
37. M. D. Krylova, I. S. Sedova, I. N. Krylov, et al., *Evolution of Material during Ultrametamorphism: Evidence from the Precambrian of Eastern Siberia* (Nauka, Leningrad, 1972) [in Russian].
38. K. Kullerud and M. Erambert, "Cl-Scapolite, Cl-Amphibole, and Plagioclase Equilibria in Ductile Shear Zones at Nusfjord, Lofoten, Norway: Implications for Fluid Compositional Evolution during Fluid–Mineral Interaction in Deep Crust," Geochim. Cosmochim. Acta. **63**, 3829–3844 (1999).
39. Yu. A. Kuznetsov and E. P. Izokh, "Geologic Evidence for Intratelluric Flows of Heat and Material," in *Problems of Petrology and Genetic Mineralogy* (Nauka, Moscow, 1969), Vol. 1, pp. 7–20 [in Russian].
40. T. L. Larikova, "Genesis of Drusitic (Corona) Textures around Olivine and Orthopyroxene during Metamorphism of Gabbroids in Northern Belomorie, Karelia," Petrologiya **8**, 430–448 (2000) [Petrology **8**, 384–401 (2000)].
41. V. V. Lashkevich, "Physicochemical Modeling of Fluid Granitizing Systems," in *Proceedings of All-Russian Symposium on Fluid Flows in the Earth's Crust and Mantle, Moscow, Russia, 2002* (Moscow, 2002), pp. 130–134 [in Russian].
42. F. A. Letnikov, "Poligenetic Fluid Flows in the Lithosphere," in *Proceedings of All-Russian Symposium on Fluid Flows in the Earth's Crust and Mantle, Moscow, Russia, 2002* (Moscow, 2002), pp. 17–22 [in Russian].
43. F. A. Letnikov, G. D. Feoktistov, N. V. Vilor, et al., *Petrology and Fluid Regime of the Continental Lithosphere* (Nauka, Novosibirsk, 1988) [in Russian].
44. F. A. Letnikov, S. O. Balyshev, V. V. Lashkevich, et al., "Interrelations among the Processes of Granitization, Metamorphism, and Tectonics," Geotektonika, No. 1, 3–22 (2000) [Geotectonics **34**, 1–18 (2000)].
45. B. G. Lutts, *Petrology of the Granulite Facies of the Anabar Massif* (Nauka, Moscow, 1964) [in Russian].
46. A. A. Marakushev, "Ascending Fluid Flows and Metallogenic Specialization of Intrusions," in *Proceedings of All-Russian Symposium on Fluid Flows in the Earth's Crust and Mantle, Moscow, Russia, 2002* (Moscow, 2002), pp. 23–26 [in Russian].
47. G. Markl, J. Ferry, and K. Bucher, "Formation of Saline Brines and Salt in the Lower Crust by Hydration Reactions and Partially Retrogressed Granulites from the Lofoten Islands, Norway," Am. J. Sci. **298**, 705–757 (1998).
48. S. S. Matveeva, "Granitization of the Ultramafic and Mafic Rocks of the Ol'khon Group, Western Baikal Area," Geokhimiya, No. 5, 707–715 (1976).
49. K. R. Mehnert, *Migmatites and the Origin of Granitic Rocks* (Elsevier, Amsterdam, 1968).
50. A. V. Milovskii, S. S. Matveeva, and E. I. Leonenko, *Granitization of Rocks* (Mosk. Gos. Univ., Moscow, 1985) [in Russian].
51. T. A. Myskova, "Conditions of Late Archean Metamorphism of the Aluminous Gneisses of the Chupa Complex in the Belomorian Province," Zap. Vseross. Miner. O–va **131** (2), 12–22 (2002).
52. R. C. Newton, "Fluids in Granulite Facies Metamorphism," Adv. Phys. Geochem. **5**, 36–59 (1986).
53. R. C. Newton, L. Y. Aranovich, E. S. Hansen, and B. A. Vandenheuvel, "Hypersaline Fluids in Precambrian Deep-Crustal Metamorphism," Precambrian Res. **91**, 41–63 (1998).
54. N. H. S. Oliver, T. J. Rawling, I. Cartwright, and P. J. Pearson, "High-Temperature Fluid–Rock Interaction and Scapolitization in an Extension-Related Hydrothermal System, Mary Kathleen, Australia," J. Petrol. **35**, 1453–1491 (1994).
55. S. N. Olsen, "Mass Balance in Migmatites," in *Migmatites*, Ed. by J. R. Ashworth (Blackie, Glasgow, 1985), pp. 145–179.
56. S. N. Olsen, "Mass Balance and Mass Transfer in Migmatites from the Colorado Front Range," Contrib. Mineral. Petrol. **85**, 30–44 (1984).
57. S. N. Olsen, "Open- and Closed-System Migmatites in the Front Range, Colorado," Am. J. Sci. **282**, 1596–1622 (1982).
58. L. L. Perchuk, "Thermodynamic Conditions of the Granitzation of Metapelitic Sequences," in *Contributions to Physicochemical Petrology* (Nauka, Moscow, 1987), Vol. 2, pp. 188–213 [in Russian].
59. L. L. Perchuk, T. V. Gerya, and L. Korsman, "Model of the Charnockitization of Gneissic Complexes," Petrologiya **2**, 451–479 (1994).

60. L. L. Perchuk, "Consistency in Some Fe–Mg Geothermometers Based on the Nernst Law: Revision," Geochem. Int. **12**, 1–11 (1989).

61. L. L. Perchuk, O. G. Safonov, T. V. Gerya, et al., "Mobility of Components in Metasomatic Transformation and Partial Melting of Gneisses: an Example from Sri Lanka," Contrib. Mineral. Petrol. **140**, 212–232 (2000).

62. Z. I. Petrova and V. I. Levitskii, *Petrology and Geochemistry of Granulite Complexes of the Baikal Region* (Nauka, Novosibirsk, 1984) [in Russian].

63. R. Powell, "Regression Diagnostics and Robust Geothermometer/Geobarometer Calibration: the Garnet–Clinopyroxene Geothermometer Revised," J. Metamorph. Geol. **3**, 327–342 (1985).

64. R. P. Rapp, "Amphibole-Out Phase Boundary in Partially Melted Metabasalt, Its Control over Liquid Fraction and Composition and Source Permeability," J. Geophys. Res. **100**, 15601–15610 (1995).

65. P. Robinson, "Metamorphosed Igneous Rocks at High Temperatures," in *Amphiboles: Petrology and Experimental Phase Relations*, Ed. by D. V. Veblen and P. H. Ribbe, Rev. Mineral. **9B**, 182–206 (1982).

66. T. Rushmer, "Partial Melting of Two Amphibolites: Contrasting Experimental Results Under Fluid-Absent Conditions," Contrib. Mineral. Petrol. **107**, 41–59 (1991).

67. I. D. Ryabchikov and A. L. Boettcher, "Experimental Evidence at High Pressure for Potassic Metasomatism in the Earth," Am. Mineral. **65**, 915–919 (1980).

68. I. D. Ryabchikov, "Fluid Regime of Mantle Plumes," Geokhimiya, No. 9, 923–927 (2003) [Geochem. Int. **41**, 838–843 (2003)].

69. I. D. Ryabchikov, "Formation Mechanism of Kimberlite Melts," in *Proceedings of International Symposium on Evolution of the Continental Lithosphere, Origin of Diamonds and Their Deposits, Novosibirsk, Russia, 2005* (Sib. Otd. Ross. Akad. Nauk, Novosibirsk, 2005), p. 65 [in Russian].

70. A. Savolahti, "On Rocks Containing Garnet, Hypersthene, Cordierite and Gedrite in the Kiuruvesi Region, Finland," Compt. Rend. Soc. Geol. Finl. **38**, 343–386 (1966).

71. M. E. Schneider and D. H. Eggler, "Fluids in Equilibrium with Peridotite Minerals: Implications for Mantle Metasomatism," Geochim. Cosmochim. Acta **50**, 711–724 (1986).

72. E. V. Sharkov, I. S. Krasivskaya, and A. V. Chistyakov, "Dispersed Mafic–Ultramafic Intrusive Magmatism in Early Paleoproterozoic Mobile Zones of the Baltic Shield: An Example of the Belomorian Drusite (Coronite) Complex," Petrologiya **12**, 632–655 (2004) [Petrology **12**, 561–582 (2004)].

73. T. F. Shcherbakova, *Amphibolites of the Belomorian Complex and Their Granitization* (Nauka, Moscow, 1988) [in Russian].

74. N. G. Sudovikov, *Regional Metamorphism and Some Petrological Problems* (Leningr. Gos. Univ., Leningrad, 1964) [in Russian].

75. N. G. Sudovikov, V. A. Glebovitskii, G. M. Drugova, et al., *Geology and Petrology of the Middle Part of the Southern Framing of the Aldan Shield* (Nauka, Moscow, 1965) [in Russian].

76. E. N. Terekhov, E. S. Przhiyalgovskii, and V. I. Levitskii, "Granulite Complex of Western Belomorian, Eastern Baltic Shield: Structural Position and Geochemical Features," Geol. Razved., No. 5, 15–30 (1997) [in Russian].

77. D. Vielzeuf and M. W. Schmidt, "Melting Relations in Hydrous Systems Revisited: Application to Metapelites, Metagreywackes and Matabasalts," Contrib. Mineral. Petrol. **141**, 251–267 (2001).

78. O. I. Volodichev, *Belomorian Complexes of Karelia: Geology and Petrology* (Nauka, Leningrad, 1990) [in Russian].

79. I. M. Volokhov and V. M. Ivanov, "Interrelations of Granitoids and Rocks of the Gabbro–Pyroxenite–Dunite Formation and Correlation with the Granitization of the Gabbroids of the Shaman Pluton of the Lysogorsk Complex, Western Sayan," in *Ore Formation and Genesis of Endogenous Deposits* (Nauka, Moscow, 1968), pp. 281–303 [in Russian].

80. T. M. Will, R. Powell, and T. J. B. Holland, "A Calculated Petrogenetic Grid for Ultramafic Rocks in the System CaO–FeO–MgO–Al_2O_3–SiO_2–CO_2–H_2O," Contrib. Mineral. Petrol. **105**, 347–358 (1990).

81. V. A. Zharikov and S. N. Gavrikova, "Granite Formation in the Active Margin of the Aldan–Stanovik Shield," Zap. Vses. Miner. O–va **116** (4), 377–399 (1987).

82. V. A. Zharikov, "Some Actual Aspects of Fluid Problem (Introduction into the Problem)," in *Proceedings of All-Russian Symposium on Fluid Flows in the Earth's Crust and Mantle, Moscow, Russia, 2002* (Moscow, 2002), pp. 11–16 [in Russian].

83. V. A. Zharikov, "Some Aspects of the Problem of Granite Formation," Vestn. Mosk. Univ., Ser. 4: Geol., No. 4, 3–13 (1996).

84. V. A. Zharikov, "Problems of Granite Formation," Vestn. Mosk. Univ., Ser. 4: Geol., No. 6, 3–14 (1987).

85. V. V. Zhdanov, "Mineral Transformations during Granitization of the Rocks of the Belomorian Complex," Inf. Sb. VSEGEI, Ser. Petrografiya., No. 7, 89–95 (1959).